ELSEVIER

# Behaviour of high field strength elements in subduction zones: constraints from Kamchatka–Aleutian arc lavas

Carsten Münker[a],[*], Gerhard Wörner[b], Gene Yogodzinski[c], Tatiana Churikova[d]

[a] Zentrallabor für Geochronologie (ZLG), Institut für Mineralogie, Corrensstr. 24, Universität Münster, Munster D-48149, Germany
[b] GZG, Abteilung Geochemie, Goldschmidtstr. 1, Universität Göttingen, 37077 Göttingen, Germany
[c] Department of Geological Sciences, University of South Carolina, Columbia, SC 29208, USA
[d] Institute of Volcanic Geology and Geochemistry, Piip Avenue 9, Petropavlovsk-Kamchatsky, Russia

## Abstract

Models explaining the characteristic depletion of High Field Strength Elements (HFSE) relative to elements of similar compatibility in subduction zone magmas invoke either (1) the presence of HFSE-rich minerals in the subduction regime or (2) a selectively lower mobility of HFSE during subduction metasomatism of the mantle. In order to investigate the properties of HFSE in subduction regimes closer, we performed high precision measurements of Nb/Ta, Zr/Hf, and Lu/Hf ratios together with $^{176}$Hf/$^{177}$Hf analyses on arc rocks from Kamchatka and the western Aleutians. The volcanic rocks of the Kamchatka region comprise compositional end members for both fluid and slab melt controlled mantle regimes, thus enabling systematic studies on the HFSE mobility at different conditions in the subarc mantle. Hf–Nd isotope and systematic Zr/Hf and Lu/Hf covariations illustrate that Zr–Hf and Lu are immobile in fluid-dominated regimes. Hf–Nd isotope compositions furthermore indicate the presence of "Indian" type depleted mantle beneath Kamchatka, as previously shown for the Mariana and Izu–Bonin arcs. In addition to a depleted mantle component, Hf–Nd isotope compositions enable identification of a more enriched mantle wedge component in the back-arc (Sredinny Ridge) that most likely consists of mantle lithosphere. The ratios of Nb/Ta and Zr/Hf are decoupled in rocks from fluid-dominated sources, indicating that Nb and Ta can be enriched in the mantle by subduction fluids to a small extent. In contrast to the fluid-dominated regime in Central Kamchatka, the budget of HFSE and Lu in rocks from the Northern Kamchatka Depression and in adakitic rocks from the western Aleutians is significantly affected by slab melts that originate from subducted oceanic crust. Compositions of the rocks with the highest slab melt components in their source (Sr/Y>30) provide no evidence that either Nb/Ta or Zr/Hf ratios are fractionated at a globally significant scale during melting of subducted oceanic crust. Subduction processes are therefore an unlikely candidate to explain the terrestrial Nb–Ta paradox (i.e., the subchondritic Nb/Ta ratios in all accessible terrestrial silicate reservoirs).

* Corresponding author. Tel.: +49-251-83-33401; fax: +49-251-83-38397.
  *E-mail address:* muenker@nwz.uni-muenster.de (C. Münker).

## 1. Introduction

In subduction-related volcanic rocks, the High Field Strength Elements (HFSE: Nb, Ta, Zr, and

Hf) display a characteristic depletion relative to the rare earth elements (REE) and large ion lithophile elements (LILE) (e.g., [1]) despite their similar compatibility during mantle melting. This depletion is the consequence of mass flux processes from the subducting plate to the subarc mantle. Most arc magmas originate from the subarc mantle wedge (e.g., [2]) which is enriched by fluids and melts from subducted oceanic crust and overlying pelagic sediments. At present-day temperature gradients in the Earth's mantle, old subducted oceanic crust typically dehydrates. In contrast to older models, arguing that old oceanic crust tends not to reach the solidus (e.g., [3]) more recent models [4] suggest that oceanic crust as old as 80 My can reach the solidus. There is general consensus that melting of subducted basaltic crust occurs in regions where very young ($<5$ My) and hot oceanic crust subducts [5,6]. Subducted pelagic sediment has a lower solidus than oceanic crust and can melt in present day subduction regimes (e.g., [7]). Some recent studies (e.g., [1,8]), have concluded that HFSE exhibit "conservative" behavior during element transfer at the slab-mantle wedge interface; that is, the abundances of HFSE in arc rocks reflect those in the mantle wedge. In contrast, LILE and light REE (LREE) have "nonconservative" properties in subduction zones due to their higher mobility relative to HFSEs in slab-derived fluids (e.g., [8,9]). More recent experimental evidence (e.g., [10,11]), however, indicates that the mobility of HFSEs during slab dehydration probably approaches that of LREEs and LILEs at increasing pressures and solute contents of the fluids. These constraints would require the presence of amphibole [12,13] or a residual titanate phase, most likely rutile [10,11], in the sources of arc magmas that selectively retain the HFSE. Models that invoke HFSE depletion by titanium phases in the sources of arc magmas therefore focus on rutile-bearing eclogite or garnet amphiblolite in deep subducting slabs (e.g., [11,14,15]). This is because rutile is unstable during peridotite melting in the mantle wedge because of its high solubility in basaltic melts [16].

Besides pure mass balance calculations (e.g., [8]), recent approaches to assess the mobility of HFSEs in subduction zones centered on combined $^{176}Hf/^{177}Hf$ and $^{143}Nd/^{144}Nd$ isotope systematics in arc rocks (e.g., [17–19]). In subduction fluids, Nd

as mobile LREE is expected to be much more mobile relative to the "conservative" Hf. Both isotope ratios would be decoupled in this case, and the pristine Hf isotope compositions of the mantle wedge would remain unmodified. The possible change of Nd isotope ratios in arc rocks would cause a shift from the global $^{176}Hf/^{177}Hf$–$^{143}Nd/^{144}Nd$ array where Hf and Nd isotope ratios are well correlated. Such a decoupling of Nd from Hf isotope ratios is indeed observed for intraoceanic arcs in the W. Pacific [18,20]. In contrast to the model of [18] who, on the basis of the Western Pacific data, argued for a conservative behaviour of Hf, the mobility of Hf in slab derived fluids was recently proposed in several studies (e.g., [19,21] and references therein). [19] argued for addition of Hf to the mantle wedge by slab derived melts and fluids because of systematic changes in Hf isotope composition along arc-back-arc traverses in W. Pacific intraoceanic arcs. In arc systems, where sediments contribute a significant portion of the trace element inventory (e.g., Antilles, Sunda-Banda) it is commonly accepted that significant amounts of Hf in the volcanic rocks derive from the sediments and not from the mantle wedge (e.g., [17,19]). Possible mechanisms include (1) addition of Hf by melts derived from subducted sediments or (2) shallow level crustal contamination.

Whereas the mobility of Hf (and Zr) in subduction zones has now been studied, the geochemical properties of Nb–Ta are yet little constrained. Recent models (e.g., [22–26]) have mostly employed Nb abundances and Nb/Ta ratios in subduction rocks to assess the possible mobility of Nb and Ta. The apparent overlap of Nb concentrations and Nb/Ta ratios with compositions of mid ocean ridge basalts (MORB) has been used in favour of a "conservative" model. As in MORB, an observed positive correlation between Nb/Ta ratios and Nb concentrations was interpreted as reflecting variable degrees of mantle depletion that is controlled by different $D_{Nb}/D_{Ta}$ in clinopyroxene (e.g., [22,27, 28]). In alternative models (e.g., [12,23,25]) correlations of Nb/Ta ratios with more mobile elements were taken as evidence that the budget of Nb and Ta might be at least partially controlled by subduction components. A further assessment of these two contrasting models was long hampered by the limi-

ted availability of Nb–Ta data of sufficient precision and accuracy.

Here we present a coherent HFSE data set for a well-characterized suite of subduction-related volcanic rocks from Kamchatka and the western Aleutians [6,29,30]. Together with $^{176}Hf/^{177}Hf$ isotope compositions the data set includes Nb/Ta, Zr/Hf, and Lu/Hf ratios that were analyzed at high precision and accuracy by multiple-collector inductively coupled plasma source mass spectrometry (MC-ICPMS) using isotope dilution [31,32]. In combination with Hf–Nd isotope systematics, the HFSE ratios are used to constrain the mobility of HFSE during subduction zone processes. This approach exploits the near identical geochemical properties of the element pairs Nb–Ta and Zr–Hf [33]. Because of these similar properties, very few petrogenetic processes are capable of fractionating the Zr–Hf and Nb–Ta pairs. Recent improvements in analytical techniques revealed variations of Nb/Ta and Zr/Hf ratios by up to 40% in different terrestrial silicate reservoirs ([34] and references therein). Amongst other hypotheses, the observed variations have been attributed to subduction processes involving rutile or amphibole [35–37]. Using the HFSE data for the Kamchatka/Aleutian rocks, we attempt (1) to assess differences in HFSE mobility during slab melting and dehydration and (2) to identify different source mineralogies. The Kamchatka–western Aleutian arcs are ideally suited for this purpose because (1) they display compositional end members for both slab fluid-and slab melt-dominated regimes in the subarc mantle and (2) subducted sediments play an insignificant role [6,30].

## 2. Geological setting and geochemistry

The Kamchatka arc is divided into three segments [38,39] of which the two southern segments from 51° to 57°N are presently active. Along the southern two segments, the Pacific Plate presently subducts beneath the Asian plate (Fig. 1). At 56°N, volcanism extends ca. 200 km across the arc. At ca. 57°N, the Kamchatka collision zone is intersected by the western Aleutian arc at an angle of ca. 90°. Beneath the western Aleutian arc (Komandorsky region) plate movement occurs in oblique strike-slip mode ([6] and references therein). Between 54° and 55°N, the
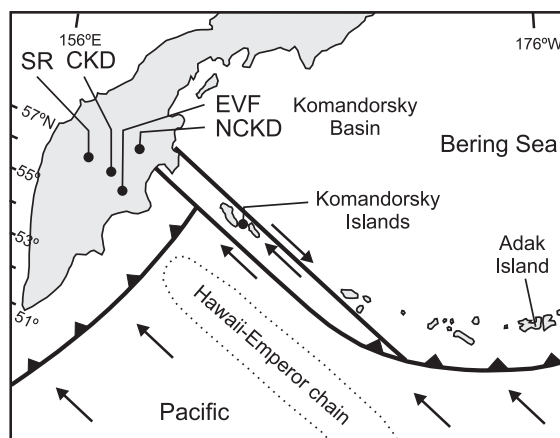


Fig. 1. Map of the Kamchatka and western Aleutian arc systems. Eastern volcanic front (EVF), central Kamchatka depression (CKD), northern central Kamchatka depression (NCKD), Sredinny Ridge (SR).

Hawaii–Emperor seamount chain (OIB) subducts beneath the Kamchatka arc. Samples examined in this study are calc-alkaline rocks from an arc traverse at 56°N [30] and from the Northern segment of the Central Kamchatka Depression (NCKD), located adjacent to the junction between the Kamchatka and Aleutian arcs at 57°N. Additional Aleutian samples include adakitic to calc-alkaline rocks from the Komandorsky basin [6] and one adakite from Adak Island in the central Aleutians [29].

Along the arc traverse at 56°N, active volcanoes in Kamchatka are divided into three groups: Eastern Volcanic Front (EVF), Central Kamchatka Depression (CKD) and Sredinny Ridge (SR) (Fig. 1), based on their location and also defined by trace element geochemistry [30,39]. Major element compositions along the 56° arc traverse are mostly basaltic to basaltic–andesitic with $SiO_2$ and MgO contents ranging from 47 to 56 wt.% and 4–10 wt.% ([30], Table 1). Two more differentiated (andesitic–dacitic) samples from the EVF were also included to assess the influence of differentiation processes on HFSE systematics. Rocks of the EVF are interpreted to originate from more depleted mantle wedge sources than those of the CKD, as indicated by ratios of conservative trace element such as Zr/Y [30,40]. In the SR, the mantle wedge composition becomes progressively enriched, as indicated from elevated

Table 1
Lu–Zr–Hf–Nb–Ta concentrations and Hf–Nd isotope compositions for the measured Kamchatka and W. Aleutian samples

| Location | Sample no. | Wt.% MgO | $^{143}$Nd/$^{144}$Nd | εNd | $^{176}$Hf/$^{177}$Hf | εHf | Zr | Hf | Nb | Ta | Lu | Zr/Nb | Zr/Hf | Nb/Ta | $^{176}$Lu/$^{177}$Hf | ΔεNd (Pearce) |
|---|---|---|---|---|---|---|---|---|---|---|---|---|---|---|---|---|
| *EVF* | | | | | | | | | | | | | | | | |
| Gamchen | GAM-07 | 5.35 | 0.513074 ± 12 | 8.5 | 0.283220 ± 10 | 15.9 | 53.47 | 1.588 | 1.09 | 0.0781 | 0.299 | 48.8 | 33.67 | 14.0 | 0.0267 | 1.4 |
| Gamchen | GAM-14 | 3.62 | *0.512991 ± 4* | 6.9 | 0.283212 ± 14 | 15.5 | 54.00 | 1.658 | 0.719 | 0.0464 | 0.349 | 75.1 | 32.57 | 15.5 | 0.0299 | 2.8 |
| Gamchen | GAM-26 | 4.94 | 0.513085 ± 12 | 8.7 | 0.283255 ± 9 | 17.1 | 50.49 | 1.547 | 0.944 | 0.0682 | 0.315 | 53.5 | 32.64 | 13.8 | 0.0289 | 2.0 |
| Gamchen | GAM-28 | 6.24 | *0.513033 ± 6* | 7.7 | 0.283235 ± 6 | 16.4 | 46.39 | 1.456 | 0.906 | 0.0552 | 0.273 | 51.2 | 31.86 | 16.4 | 0.0266 | 2.5 |
| Kizimen | KIZ-01 split 1 | 2.44 | – | – | 0.283261 ± 9 | 17.3 | 62.64 | 2.049 | 3.33 | 0.293 | 0.277 | 18.8 | 30.57 | 11.3 | 0.0192 | – |
| Kizimen | KIZ-01 split 1 | 2.44 | – | – | – | – | 62.26 | 2.045 | 3.29 | 0.290 | 0.276 | 18.9 | 30.44 | 11.3 | 0.0192 | – |
| Kizimen | KIZ-01 split 2 | 2.44 | 0.513107 ± 10 | 9.1 | 0.283272 ± 9 | 17.7 | 62.97 | 2.047 | 3.35 | 0.291 | 0.274 | 18.8 | 30.77 | 11.5 | 0.0190 | 1.9 |
| Kizimen | KIZ-19 | 5.22 | 0.513118 ± 13 | 9.4 | 0.283235 ± 10 | 16.4 | 96.15 | 2.742 | 3.61 | 0.231 | 0.439 | 26.7 | 35.07 | 15.6 | 0.0227 | 0.9 |
| Kizimen | KIZ-24 | 4.16 | *0.513048 ± 5* | 8.0 | 0.283247 ± 7 | 16.8 | 81.17 | 2.356 | 2.73 | 0.201 | 0.347 | 29.8 | 34.44 | 13.6 | 0.0209 | 2.5 |
| Kizimen | KIZ-24/1 | 4.42 | *0.513047 ± 5* | 8.0 | 0.283251 ± 9 | 16.9 | 79.63 | 2.301 | 2.51 | 0.167 | 0.371 | 31.7 | 34.62 | 15.1 | 0.0229 | 2.6 |
| Shmidt | SHM-01 | 8.07 | *0.513070 ± 6* | 8.4 | 0.283262 ± 9 | 17.3 | 68.16 | 1.986 | 1.33 | 0.102 | 0.357 | 51.4 | 34.33 | 13.0 | 0.0255 | 2.4 |
| Shmidt | SHM-03 | 2.21 | 0.513137 ± 14 | 9.7 | 0.283292 ± 9 | 18.4 | 57.20 | 1.633 | 0.940 | 0.0681 | 0.337 | 60.8 | 35.04 | 13.8 | 0.0293 | 1.8 |
| Shmidt | SHM-04 | 6.91 | *0.513032 ± 4* | 7.7 | 0.283262 ± 9 | 17.3 | 51.96 | 1.567 | 1.16 | 0.0804 | 0.290 | 44.7 | 33.15 | 14.4 | 0.0262 | 3.2 |
| Komarov | KOM-02/2 | 7.33 | *0.513036 ± 7* | 7.8 | 0.283231 ± 10 | 16.2 | 77.86 | 2.276 | 1.35 | 0.0978 | 0.332 | 57.9 | 34.21 | 13.8 | 0.0207 | 2.4 |
| Komarov | KOM-06 | 8.20 | *0.513044 ± 5* | 7.9 | 0.283211 ± 8 | 15.5 | 64.79 | 1.931 | 1.16 | 0.0792 | 0.309 | 5.7 | 33.56 | 14.7 | 0.0227 | 1.8 |
| *CKD* | | | | | | | | | | | | | | | | |
| Kluchevskoy | KLU-03 | 8.88 | *0.513080 ± 6* | 8.6 | 0.283244 ± 12 | 16.7 | 70.27 | 2.019 | 1.39 | – | 0.260 | 50.6 | 34.81 | – | 0.0183 | 1.8 |
| Kluchevskoy | KLU-03 | 8.88 | 0.513104 ± 10 | 9.1 | 0.283272 ± 10 | 17.7 | 70.14 | 2.026 | 1.35 | 0.0925 | 0.260 | 51.8 | 34.61 | 14.6 | 0.0182 | 2.0 |
| Kluchevskoy | KLU-06 | 8.33 | *0.513070 ± 6* | 8.4 | 0.283275 ± 13 | 17.8 | 72.80 | 2.100 | 1.38 | 0.0973 | 0.273 | 52.9 | 34.67 | 14.2 | 0.0184 | 2.7 |
| Kluchevskoy | KLU-12 | 5.03 | *0.513102 ± 6* | 9.1 | 0.283276 ± 9 | 17.8 | 95.58 | 2.670 | 1.86 | 0.125 | 0.343 | 51.4 | 35.80 | 14.8 | 0.0182 | 2.1 |
| Kluchevskoy | KLU-15 | 8.67 | *0.513109 ± 7* | 9.2 | 0.283226 ± 8 | 16.1 | 67.53 | 1.938 | 1.34 | 0.0890 | 0.284 | 50.5 | 34.85 | 15.0 | 0.0208 | 0.9 |
| Ploskie Sopky | 2330 | 7.97 | *0.513078 ± 6* | 8.6 | 0.283236 ± 7 | 16.4 | 69.87 | 2.071 | 1.44 | 0.0981 | 0.304 | 48.6 | 33.74 | 14.7 | 0.0208 | 1.7 |
| Ploskie Sopky | 3-90 | 7.84 | *0.513069 ± 6* | 8.4 | 0.283224 ± 9 | 16.0 | 60.10 | 1.788 | 1.17 | 0.0770 | 0.243 | 51.2 | 33.61 | 15.2 | 0.0193 | 1.6 |
| Tolbachik | TOL-96-01 | 4.67 | 0.513141 ± 5 | 9.8 | 0.283267 ± 9 | 17.5 | 204.3 | 5.211 | 5.16 | 0.360 | 0.518 | 39.6 | 39.21 | 14.3 | 0.0141 | 1.1 |
| Tolbachik | TOL-96-03 | 9.10 | *0.513081 ± 5* | 8.6 | 0.283271 ± 10 | 17.7 | 118.4 | 3.175 | 2.92 | 0.197 | 0.364 | 40.5 | 37.30 | 14.8 | 0.0163 | 2.4 |
| *NCKD* | | | | | | | | | | | | | | | | |
| Kharchinsky | 8840 | 11.3 | 0.513095 ± 12 | 8.9 | 0.283255 ± 3 | 17.1 | 65.75 | 2.005 | 1.18 | 0.0764 | 0.224 | 55.8 | 32.79 | 15.4 | 0.0158 | 1.8 |
| Zarechny | 90093 | 10.4 | *0.513112 ± 5* | 9.2 | 0.283253 ± 10 | 17.0 | 62.23 | 1.899 | 1.16 | 0.0818 | 0.255 | 53.7 | 32.77 | 14.2 | 0.0190 | 1.4 |
| Shiveluch | 2569 | 7.01 | *0.513114 ± 8* | 9.3 | 0.283257 ± 9 | 17.2 | 77.51 | 2.213 | 1.86 | 0.125 | 0.246 | 41.6 | 35.02 | 14.9 | 0.0158 | 1.4 |
| Shiveluch | 2577 | 6.78 | 0.513138 ± 10 | 9.8 | 0.283258 ± 11 | 17.2 | 74.76 | 2.219 | 1.37 | 0.0900 | 0.301 | 54.5 | 33.68 | 15.3 | 0.0192 | 1.0 |
| Shiveluch | 2581 | 8.18 | 0.513058 ± 13 | 8.2 | 0.283246 ± 8 | 16.8 | 76.84 | 2.199 | 1.75 | 0.119 | 0.244 | 43.9 | 34.94 | 14.7 | 0.0157 | 2.3 |
| Shiveluch | 2585 | 7.42 | *0.513124 ± 6* | 9.5 | 0.283248 ± 10 | 16.8 | 75.31 | 2.161 | 1.72 | 0.111 | 0.242 | 43.9 | 34.84 | 15.4 | 0.0159 | 1.0 |
| Shiveluch | 5734 | 12.1 | *0.513059* | 8.2 | 0.283231 ± 8 | 16.2 | 88.56 | 2.518 | 1.76 | 0.112 | 0.276 | 50.4 | 35.17 | 15.7 | 0.0156 | 1.9 |
| Shiveluch | SHIV-01-01 | 3.57 | 0.513157 ± 6 | 10.1 | 0.283259 ± 8 | 17.2 | 89.37 | 2.534 | 1.69 | 0.121 | 0.183 | 52.8 | 35.27 | 14.0 | 0.0102 | 0.6 |
| Shiveluch | SHIV-01-05 | 5.61 | 0.513138 ± 13 | 9.8 | 0.283254 ± 6 | 17.1 | 88.81 | 2.486 | 1.63 | 0.112 | 0.292 | 54.4 | 35.72 | 14.6 | 0.0167 | 0.9 |
| Shiveluch | SHIV-01-12 | 3.73 | 0.513142 ± 10 | 9.8 | 0.283259 ± 9 | 17.2 | 91.45 | 2.582 | 1.81 | 0.128 | 0.188 | 50.4 | 35.42 | 14.2 | 0.0104 | 0.9 |

| Location | Sample no. | Wt.% MgO | $^{143}$Nd/$^{144}$Nd | εNd | $^{176}$Hf/$^{177}$Hf | εHf | Zr | Hf | Nb | Ta | Lu | Zr/Nb | Zr/Hf | Nb/Ta | $^{176}$Lu/$^{177}$Hf | ΔεNd (Pearce) |
|---|---|---|---|---|---|---|---|---|---|---|---|---|---|---|---|---|
| *SR* | | | | | | | | | | | | | | | | |
| Achtang | ACH-01 | 5.13 | 0.513039 ± 6 | 7.8 | 0.283184 ± 6 | 14.6 | 117.6 | 3.040 | 5.76 | 0.369 | 0.285 | 20.4 | 38.70 | 15.6 | 0.0133 | 1.3 |
| Esso | ESO-08 | 6.51 | *0.513092 ± 6* | 8.9 | 0.283248 ± 9 | 16.8 | 63.59 | 1.851 | 1.53 | 0.0967 | 0.236 | 41.6 | 34.36 | 15.8 | 0.0181 | 1.7 |
| Ichinsky | ICH-02 | 4.80 | *0.513046 ± 7* | 8.0 | 0.283156 ± 8 | 13.6 | 176.4 | 4.265 | 8.23 | 0.463 | 0.371 | 21.4 | 41.35 | 17.8 | 0.0123 | 0.5 |
| Ichinsky | ICH-05 | 7.38 | *0.512987 ± 5* | 6.8 | 0.283110 ± 8 | 12.0 | 141.4 | 3.397 | 17.8 | 1.019 | 0.268 | 7.95 | 41.64 | 17.5 | 0.0112 | 0.7 |
| Ichinsky | ICH-10 | 8.64 | *0.512974 ± 6* | 6.5 | 0.283152 ± 8 | 13.4 | 142.2 | 3.440 | 16.8 | 1.009 | 0.274 | 8.49 | 41.35 | 16.6 | 0.0113 | 1.9 |
| Ichinsky | ICH-69 | 6.94 | 0.513021 ± 7 | 7.5 | 0.283192 ± 4 | 14.9 | 154.2 | 3.802 | 11.6 | 0.663 | 0.340 | 13.3 | 40.57 | 17.5 | 0.0127 | 1.8 |
| *W. Aleutians* | | | | | | | | | | | | | | | | |
| Komandorsky | 8-4-78 | 2.16 | 0.513113 ± 10 | 9.3 | 0.283211 ± 7 | 15.5 | 94.4 | 2.689 | 4.11 | 0.343 | 0.125 | 23.0 | 35.10 | 12.0 | 0.0066 | 0.4 |
| Komandorsky | 8-6-78 | 2.89 | 0.513093 ± 10 | 8.9 | 0.283225 ± 10 | 16.0 | 86.5 | 2.316 | 3.20 | 0.271 | 0.123 | 27.1 | 37.34 | 11.8 | 0.0076 | 1.1 |
| Komandorsky | KCP/Y1 | 5.54 | 0.513079 ± 11 | 8.6 | 0.283212 ± 9 | 15.6 | 100.2 | 2.770 | 3.30 | 0.210 | 0.110 | 30.4 | 36.19 | 15.7 | 0.0057 | 1.1 |
| Adak Island | ADK-53 | 5.58 | 0.513089 ± 11 | 8.8 | 0.283205 ± 10 | 15.3 | 100.6 | 2.762 | 2.82 | 0.172 | 0.209 | 35.7 | 36.44 | 16.4 | 0.0107 | 0.8 |
| Komandorsky | V38/42Y3 | 4.44 | 0.513087 ± 19 | 8.8 | 0.283235 ± 11 | 16.4 | 157.6 | 4.111 | 3.26 | 0.190 | 0.0762 | 48.3 | 38.33 | 17.2 | 0.0026 | 1.5 |
| *Reference samples* | | | | | | | | | | | | | | | | |
| | BB (n = 11) | – | – | – | – | – | 193 ± 1.1% | 4.83 ± 0.8% | 58.4 ± 3.7% | 3.42 ± 1.7% | 0.232 ± 1.1% | 3.29 ± 3.7% | 39.9 ± 0.7% | 17.1 ± 3.5% | 0.00680 ± 0.9% | – |
| | BIR-1 (n = 6) | – | – | – | – | – | 14.0 ± 1.3% | 0.581 ± 1.5% | 0.549 ± 3.6% | 0.0350 ± 3.0% | 0.244 ± 1.0% | 25.2 ± 2.2% | 24.1 ± 0.7% | 15.8 ± 2.8% | 0.0600 ± 1.0% | – |

MgO concentration and Nd isotope data in italics are from [6,30]. All other Nd isotope ratios marked with an asterisk were measured using the VG54 TIMS at ZLG Münster. $^{143}$Nd/$^{144}$Nd results were normalized to $^{146}$Nd/$^{144}$Nd of 0.7219, an average $^{143}$Nd/$^{144}$Nd value of 0.511860 was obtained for the La Jolla standard at the time of measurement. εHf values were calculated relative to a CHUR value of 0.282772 for $^{176}$Hf/$^{177}$Hf [93], εNd are given relative to a CHUR value of 0.512638 [94]. Standard data for the BB, and BIR-1 basalts are given with 2σ r.s.d.. Within the uncertainties of previously used methods, the HFSE and Lu concentration data obtained by isotope dilution compare well with recommended values (see [32] and references therein) but are of much higher precision and accuracy.
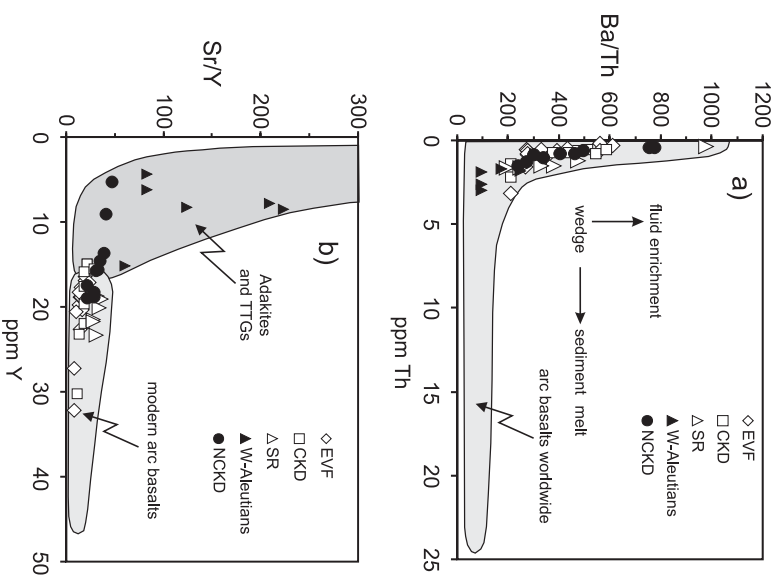
Nb–Ta concentrations, higher Ta/Yb and lower εNd. Based on nonconservative trace element and Sr–Nd–Pb isotope systematics, the magma compositions along the traverse at 56° can be explained by addition of slab derived fluids derived from subducting oceanic crust to a mantle wedge of variable composition [30,40]. Lead isotope compositions are confined to low $^{207}$Pb/$^{204}$Pb, showing no correlation between Pb-isotopes and fluid mobile elements [41]. Hence, any significant addition of subducted pelagic sediments to the mantle wedge or shallow level crustal contamination can be ruled out. The Kamchatka rocks along the 56° traverse are therefore a representative end member for a fluid-dominated subarc mantle regime. This is also shown in Ba/Th vs. Th space (Fig. 2a), where the Kamchatka samples cover the whole compositional range of other fluid-dominated intraoceanic arcs.



Fig. 2. Kamchatka arc rocks in comparison to other arc systems in (a) Ba/Th vs. Th and (b) Sr/Y vs. Y space. Arc compilations are from [5,76].

At the intersection of the Kamchatka and Aleutian arcs, the subducting Pacific plate tears along the junction of the two arc systems [42]. Volcanism in the northernmost active Kamchatka volcanoes (NCKD) is dominated by andesitic rocks interpreted to contain a slab melt component (high Sr/Y, Fig. 2b). Major element compositions in the analyzed NCKD samples range from 51 to 61 wt.% $SiO_2$ and 3–12 wt.% MgO ([30] and unpublished data, Table 1). The occurrence of adakitic melts (i.e., pristine melts from the subducting slab), however, is restricted to the western Aleutians. Because the subducting plate along the junction of the Aleutian and Kamchatka arcs is old and relatively cold, the presence of adakites in this region is explained by melting along the edges of the torn subducting plate [42]. Major element compositions in the analyzed W. Aleutian samples (Komandorsky and Adak islands) range from 56 to 66 wt.% $SiO_2$ and from 2 to 5 wt.% MgO ([6], Table 1). In particular the extremely radiogenic $\varepsilon$Nd (>+8) and the low $^{207}Pb/^{204}Pb$ [6,30,39,43] rule out any significant addition of melts from subducted pelagic sediment to the mantle wedge. Likewise, shallow level crustal contamination is probably insignificant, given the mafic nature of the rocks (Fo# up to 92) and their MORB-like isotopic compositions [30]. Trace element compositions of NCKD and western Aleutian rocks therefore allow valuable insights into melting of subducted basaltic crust.

## 3. Methods and results

A total of 43 Samples along the arc transect at 56° (EVF, CKD, SR) and from the NCKD were analyzed for their $^{176}Hf/^{177}Hf$ isotope composition and Lu–Zr–Hf–Nb–Ta concentrations (Table1). Major, trace element and Nd isotope compositions are taken from [6,30], where a detailed description of the sample suite is also given. Hf isotope and Lu–Zr–Hf–Nb–Ta concentration measurements were performed on the same (ca. 100 mg) split of sample powder. For some samples, Nd and Sr isotope compositions were additionally analyzed in the sample split. All results agreed with those of [6,30] to better than 50 ppm. The full analytical procedure for HFSE and Lu concentration measurements is de-

scribed in [31,32]. All samples were spiked using a mixed $^{180}Ta–^{180}Hf–^{176}Lu–^{94}Zr$ tracer that was calibrated against >99.9% pure Ames metals. A Lu-rich HREE fraction, Ta, Hf, and a quantitative Zr/Nb cut were separated from the whole rock matrix by ion exchange. The concentrations of Lu, Zr, Hf, and Ta were measured by isotope dilution using the Isoprobe MC-ICPMS at ZLG Münster. The concentration of Nb (monoisotopic) was measured as Zr/Nb against a Zr/Nb standard prepared from >99.9% pure Ames metals. The Nb concentration is calculated from the measured Zr/Nb using the Zr concentration obtained by isotope dilution. External precision and accuracy as determined by multiple digestions of different rock matrices (Table 1 and [32]) are better than ± 4% for Nb/Ta, ± 0.6% for Zr/Hf, and ± 1% for Lu/Hf (all $2\sigma$ r.s.d.). These reproducibilities are also confirmed by replicate measurements of two Kamchatka samples (KIZ-01, KLU-03, Table 1). Hf isotope measurements at ZLG Münster were performed using the method described in [31]. After normalization to a $^{179}Hf/^{177}Hf$ of 0.7325 (exponential law), an average $^{176}Hf/^{177}Hf$ value of 0.282140 was obtained for the Münster AMES metal standard that is isotopically indistinguishable from the JMC-475 standard. All Hf isotope results in Table1 are reported relative to a $^{176}Hf/^{177}Hf$ value of 0.282160. The external reproducibility for $^{176}Hf/^{177}Hf$ was ± 50 ppm ($2\sigma$).

Hafnium isotope compositions of the Kamchatka rocks vary between +12 and +18 $\varepsilon$-units. Rocks from the EVF, CKD, and NCKD show little variation in their $\varepsilon$Hf (+15.5 to +18). Ratios for the SR rocks (+12 to +17) extend to lower $\varepsilon$Hf, consistent with a proposed OIB source component in the mantle source of these magmas [30]. In $\varepsilon$Hf–$\varepsilon$Nd space, the Kamchatka samples overlap with the terrestrial mantle array (Fig. 3a). Many EVF samples, however, are displaced to lower $\varepsilon$Nd relative to the trend defined by the CKD, NCKD and SR samples, suggesting some selective addition of slab-derived Nd to the mantle wedge beneath the arc front. The western Aleutian samples are slightly displaced from the Kamchatka array to lower $\varepsilon$Hf (+15 to +16.5) at the center of the broadly defined MORB field (Fig. 3b).

With few exceptions in the EVF (Gamchen) and SR (Ichinsky), the measured Nb/Ta and Zr/Hf ratios

in the Kamchatka arc rocks and those of present day MORB overlap ([44,45] and Fig. 4). Rocks of the EVF, CKD and NCKD display Nb/Ta ratios between 13 and 16.5, excluding one dacitic outlier (KIZ-01). In contrast to these three suites, the SR samples display higher Nb/Ta ratios up to 18. The Aleutian samples display more variable Nb/Ta ratios of 11–17. Measured Zr/Hf and $^{176}Lu/^{177}Hf$ ratios range from 30.6 to 41.6 and from 0.002 to 0.030, respectively. Along the arc traverse at 56°, both ratios are inversely correlated (Fig. 4a), Lu/Hf decreases from the EVF to the SR and Zr/Hf increases. Samples from the western Aleutians are significantly displaced from this array to lower Lu/Hf ratios. The NCKD samples fall in an intermediate position between the Aleutian and EVF samples. In all suites, Zr/Hf ratios are also positively correlated with the Zr abundances (Fig. 4b), suggesting that the effects of crystal fractionation on incompatible trace element abundances and ratios are minor. No clear correlation is observed between Nb/Ta and Zr/Hf ratios (Fig. 4c). In samples with less than ca. 60 wt.% $SiO_2$, neither Nb/Ta nor Zr/Hf ratios are correlated with $SiO_2$ (not shown). This confirms that both ratios are little modified during crystal fractionation in basalts and andesites, consistent with earlier observations [25,44]. Significantly lower Nb/Ta and Nb/La ratios in the dacitic sample KIZ-01 (63.6% $SiO_2$) can be explained by fractionation of low-Mg amphibole that has $D_{Nb}/D_{Ta}$ and $D_{Nb}/D_{La}$ of >1 [13], in marked contrast to the dacitic W. Aleutian samples (8478, 8678, high Nb/La at low Nb/Ta). Sample KIZ-01 is therefore excluded in the discussion below because the Nb/Ta
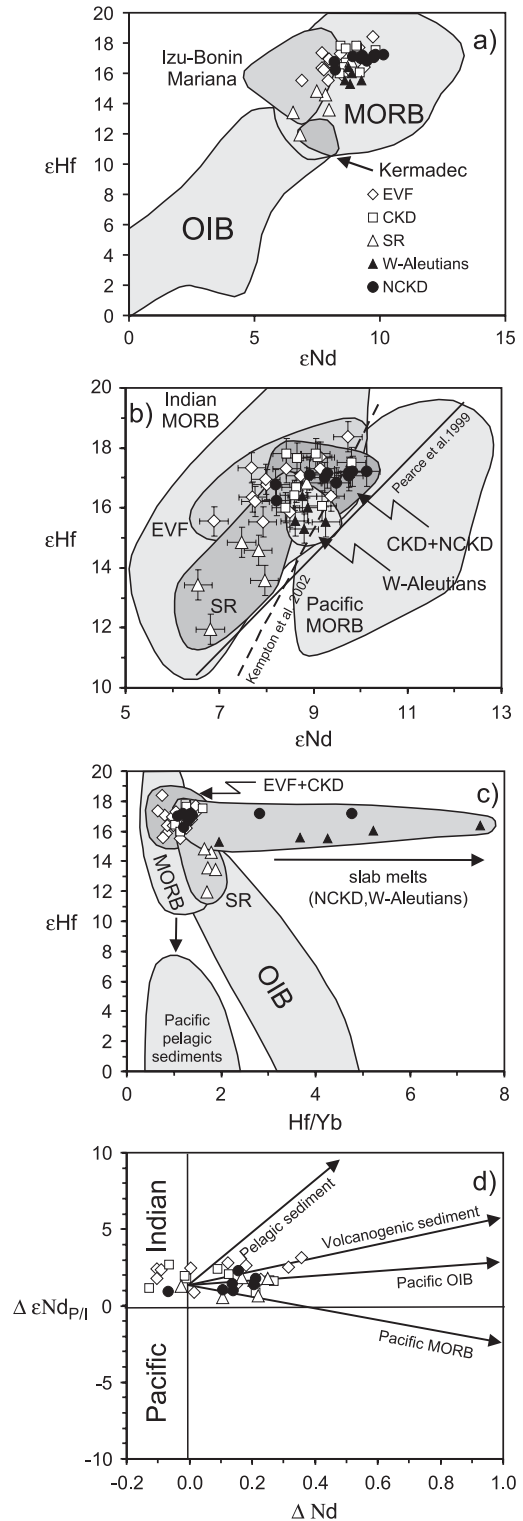


Fig. 3. (a–b) εHf vs. εNd of Kamchatka and western Aleutian arc rocks in comparison to other W. Pacific arcs and Pacific/Indian MORB [18,19,46,77]. Discrimination lines between Pacific and Indian MORB are those of [18,77], (c) εHf vs. Hf/Yb systematics in comparison to global MORB, OIB and Pacific pelagic sediment [18], (d) $\Delta\varepsilon Nd_{P/I}$ vs. $\Delta Nd$ projection for the Kamchatka and Aleutian arc rocks. Note that some adakitic samples from the Aleutians display positive Hf anomalies, resulting in $\Delta Nd$ below −0.2 (plotting off the diagram). Vectors indicate addition of fluids derived from subducted pelagic/volcanogenic sediments and Pacific OIB/MORB and are those of [18]. $\Delta\varepsilon Nd_{P/I}$ is calculated relative to the Pacific/Indian mantle domain discrimination line of [18]. Equations are $\Delta\varepsilon Nd_{P/I} = 0.625\varepsilon Hf - \varepsilon Nd$ and $\Delta Nd = [(Nd/Yb) - 10^{(0.674 + 1.414\log(Hf/Yb))}]/[Nd/Yb]$ [18].
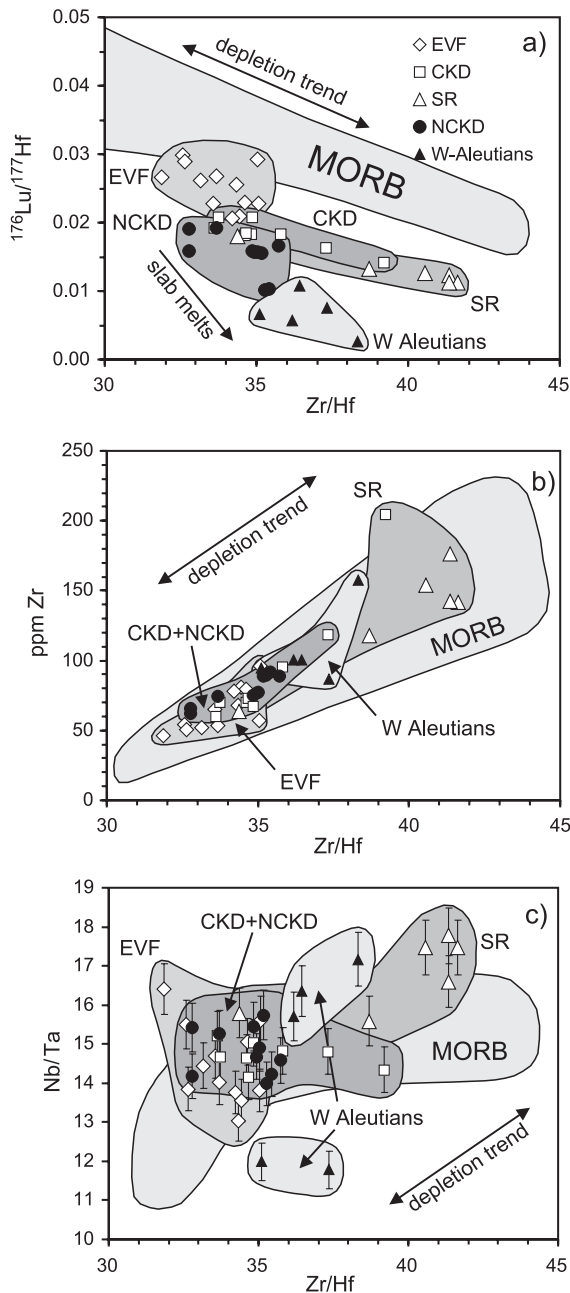
Fig. 4. Plots of (a) Lu/Hf vs. Zr/Hf, (b) Zr vs. Zr/Hf, and (c) Nb/Ta vs. Zr/Hf for the Kamchatka and western Aleutian samples in comparison to MORB. Arrows indicate depletion trends as predicted from experimental partitioning data (compatibility order Nb < Ta < Zr < Hf < Lu, references in Fig. 7). MORB data are combined high precision Nb/Ta, Zr/Hf and Lu/Hf data obtained by isotope dilution ([34,45] and unpublished data).

and possibly the Zr/Hf ratios are different to those in the parent melt.

## 4. Discussion

### 4.1. Hf–Nd isotope and element variations

A comparison of the Kamchatka/western Aleutian arc rocks with other arc systems indicates that they are comparable to other W. Pacific intraoceanic arcs (e.g., Mariana, Izu Bonin, Kermadec, Fig. 3a) in that they display extremely "depleted" Hf isotope ratios, similar to those of MORB [46]. In $\varepsilon$Hf vs. Hf/Yb space (Fig. 3c), all EVF and CKD samples overlap fields for MORB (and NW Pacific arcs) whereas some NCKD samples and the western Aleutian samples are displaced to higher Hf/Yb at similar Hf isotope compositions. The higher Hf/Yb ratios are consistent with a proposed slab melt component (high Hf/Yb) in the sources of these magmas [30,39,42] by which Hf has preferentially been added to the mantle wedge. As there is no shift in $^{176}$Hf/$^{177}$Hf with increasing Hf/Yb (Fig. 3c), both the mantle wedge and the source of the slab melt component (in this case the subducting Pacific plate) are implied to have similarly depleted Hf isotope compositions. This is also observed for Nd isotopes, where $\varepsilon$Nd in the CKD and NCKD cover the same range. Because of the similar Hf–Nd isotope compositions to the mantle wedge, coupled Hf–Nd isotope compositions alone are therefore not suitable tracers for slab-derived melts that originate from subducted oceanic crust.

The signature of subducted sediment and OIB mantle components are often geochemically similar and may be difficult to distinguish (e.g., Marianas [23,47]). For the SR samples, $\varepsilon$Nd–$\varepsilon$Hf together with $\varepsilon$Hf–Hf/Yb covariations (Fig. 3b–c) enable this discrimination. In $\varepsilon$Hf–Hf/Yb space, $\varepsilon$Hf ratios of the SR samples only decrease moderately with increasing Hf/Yb, rather suggesting addition of an enriched OIB source type mantle component. Addition of components derived from pelagic Pacific sediment to the mantle wedge would result in a more pronounced decrease in $\varepsilon$Hf (Fig. 3c). The moderate decrease of $\varepsilon$Hf with increasing Hf/Yb could also be explained by addition of a mixture of pelagic sediment and volcanogenic sediment (more radiogenic $\varepsilon$Hf [18]) or by

melts from subducted pelagic sediment that have elevated Hf/Yb. Both cases appear to be unlikely in the SR back-arc setting because the uniform, MORB-like Pb isotope ratios along the $56°$ transect [30,43] argue against pelagic sediment (elevated $^{207}Pb/^{204}Pb$ would be expected).

Because the addition of components derived from subducted pelagic sediment to the subarc mantle wedge is deemed to be insignificant, the observed Hf–Nd variations in the Kamchatka rocks can be used to infer depleted mantle compositions beneath the Kamchatka arc. Fig. 3d shows a plot of $\Delta\varepsilon Nd_{P/I}$ vs. $\Delta Nd$ for all analyzed Kamchatka samples. The $\Delta Nd$ value denotes the selective enrichment of Nd relative to Hf in the mantle wedge by subduction components. More positive values indicate a larger Nd enrichment or a larger negative Hf anomaly in an extended REE plot [18]. Both elements are little fractionated during mantle melting because they have a similar compatibility. In $\varepsilon Hf$–$\varepsilon Nd$ space, the $\Delta\varepsilon Nd_{P/I}$ value denotes the offset of a sample from the discrimination line between the Pacific and Indian mantle domains proposed by [18]. Positive $\Delta\varepsilon Nd_{P/I}$ values indicate less radiogenic $\varepsilon Nd$ at a given $\varepsilon Hf$. The proposed isotopic boundary between the Pacific and Indian mantle domains is based on the observation that MORBs from the Indian–Australian plate generally display more unradiogenic $\varepsilon Nd$ than Pacific MORBs at a given $\varepsilon Hf$ (see also Fig. 3b). [18] have previously reported the presence of "Indian" type mantle domain in the mantle wedge beneath the Izu–Bonin and Mariana arc systems which are located south of the Kamchatka arc. As rocks in these two arc systems, all of the examined Kamchatka samples also plot above the discrimination line of [18] in the Indian MORB field (Fig. 3b), implying that the Kamchatka rocks all originate from "Indian" type mantle sources. The Aleutian samples are displaced from the Kamchatka samples towards the Pacific MORB field, most likely reflecting the contribution of slab melts from the subducting Pacific plate. In Fig. 3d, the lack of a systematic increase of $\Delta\varepsilon Nd_{P/I}$ with $\Delta Nd$ in the EVF, CKD, NCKD, and SR rules out any significant addition of subducted pelagic sediment. The observed $\Delta\varepsilon Nd_{P/I}$ vs. $\Delta Nd$ relationships rather suggest a predominant role of fluids derived from subducted Pacific OIB or from a mixture of Pacific MORB and subducted volcano-

genic sediment. Most importantly, samples with no Nd enrichment (i.e., $\Delta Nd \sim 0$) still display positive $\Delta\varepsilon Nd_{P/I}$, thus confirming the presence of Indian type mantle beneath the Kamchatka arc.

The mantle wedge beneath Kamchatka is even more depleted than MORB mantle which has tentatively been attributed to the previous arc magmatism, including extensive Plio-Pleistocene plateau andesites [30]. Our combined Lu–Hf and $^{176}Hf/^{177}Hf$ data can help to test this hypothesis and to estimate both age and degree of depletion in the mantle wedge. In subduction regimes, both Lu and Hf are typical conservative elements as shown above for Hf along the $56°$ traverse in Kamchatka suites. Lutetium, however, is more compatible during mantle melting than Hf. Lu/Hf ratios decrease from the EVF to the CKD, NCKD and SR, consistent with the previously reported decrease in mantle depletion from E to W (e.g., [30]). As the average degrees of melting of all examined suites are similar ($\sim 5\%$ for the SR, $\sim 10\%$ for the CKD, $\sim 20\%$ for the EVF [30]), the observed range of Lu/Hf fractionations ($\sim 200$ %) cannot be caused by melting processes alone that produced these magmas. Except for the SR samples, there is no significant change in $^{176}Hf/^{177}Hf$ with the Lu/Hf ratios of the magmas. Rocks of the SR show a decrease of $^{176}Hf/^{177}Hf$ with decreasing Lu/Hf and 1/Hf (not shown), indicating admixture of a more enriched mantle component as evident from $\varepsilon Hf$ vs. Hf/Yb and Pb isotope systematics (Fig. 3c).

Similar $^{176}Hf/^{177}Hf$ in the CKD, NCKD and EVF magmas coupled with a 200% variation in the Lu/Hf ratio indicate a young Lu/Hf fractionation event in the mantle sources in addition to its MORB source-type depletion. If the Lu/Hf ratios of the mantle sources are calculated, these values can be used to estimate a maximum age of Lu/Hf fractionation from the maximum spread of observed Hf isotope compositions. This age corresponds to the age of the variable mantle depletion observed across the Kamchatka arc. The major source of uncertainty in such an approach is the assumption that the different magma sources initially all had the same Hf isotope composition. The possible presence of garnet at lower pressures in hydrous regimes [48], the melting model or the modal compositions of the mantle sources are of minor significance in this case. The Lu/Hf ratios of the mantle sources are
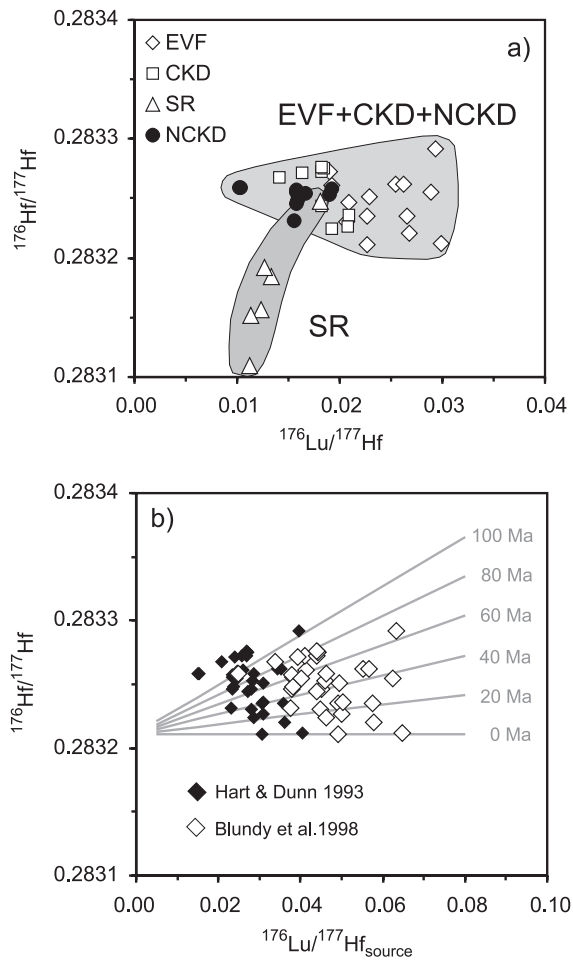
Fig. 5. Lu/Hf Isochron plot for (a) all Kamchatka arc rocks and (b) calculated mantle sources for the EVF, CKD and SR rocks. Gray lines indicate the calculated slopes for mantle depletion events at 20, 40, 60, 80, and 100 Ma, assuming a uniform initial $^{176}$Hf/$^{177}$Hf of 0.283210 in all reservoirs. Clinopyroxene is assumed as the major phase controlling the Lu/Hf fractionation during melting (e.g., [56]). Simple batch melting was assumed, the $D_{Lu}/D_{Hf}$ used for clinopyroxene are end member values taken from [49] (♦) and [50] (◇).

therefore estimated from the measured Lu/Hf ratios in the magmas (Fig. 5), assuming a simple batch melting model and a garnet-free mantle residue (also indicated from HREE abundances in the samples from the EVF-SR traverse). In this case, the bulk partition coefficient of the mantle source is approximated by that of clinopyroxene. Partition coefficients used are those of [49,50], covering the whole range of published

$D_{Lu}/D_{Hf}$ in hydrous and anhydrous regimes (e.g., [51] and references therein). Following Fig. 5, the maximum depletion age is constrained to $\sim 80$–$100$ Ma, suggesting that the regional gradient in mantle depletion was indeed established in Late Tertiary to Early Pleistocene time, when large volumes of flood basalts were erupted in Kamchatka.

Altogether, $\varepsilon$Nd–$\varepsilon$Hf constraints indicate that Nd was added to the sources of some Kamchatka magmas (in particular beneath the EVF), whereas Hf was conservative. The Hf–Nd isotope composition of the mantle wedge beneath Kamchatka is similar to that of the "Indian" type mantle domain. A previously identified additional enriched mantle component, comparable to that of OIB or enriched lithospheric mantle can be confirmed in the source of the SR magmas. Hf–Nd isotope compositions in the magmas of the NCKD and western Aleutians are a mixture of those from the subducting Pacific plate and mantle wedge material.

## 4.2. Properties of Zr–Hf and heavy rare earth elements (HREE)

Covariations of Zr–Hf and HREE enable a further assessment of the subduction zone mobility of Zr, Hf, and Lu. It is claimed from mass balance calculations for other fluid-dominated intraoceanic arc regimes (e.g. Marianas, Izu Bonin, South Sandwich, and N Toga Kermadec arcs [23,52,53]) that the HREE exhibit conservative properties, i.e., that they are not enriched by subduction components. A conservative behaviour of the HREE is also evident for most suites of the Kamchatka arc. Except for the NCKD and western Aleutian rocks, most analyzed suites display similar ranges of HREE concentrations that are up to a factor of 3 lower than those of N-MORB. The similarity of HREE abundances also indicates similar conditions of partial melting and degrees of fractionation for all analyzed Kamchatka samples (following [30,54]). This is also supported by a coupled increase of Zr concentrations with Zr/Hf ratios (Fig. 4b). If the magmas melted and crystallized under very different conditions, the element abundances of Zr and Hf would shift whereas the Zr/Hf ratio would be little modified.

In Lu/Hf vs. Zr/Hf space (Fig. 4a), the Kamchatka samples from the EVF, CKD and SR form an inversely correlated array. The NCKD and western Aleutian magmas are displaced from this array to lower and

three samples from the EVF (Shmidt, Gamchen) to slightly higher Lu/Hf ratios. The major Lu/Hf vs. Zr/Hf array confirms a relative compatibility order of Zr < Hf < Lu during clinopyroxene (and garnet) controlled mantle melting (e.g., [49,55,56]). The more hydrous melting conditions in the subarc mantle wedge therefore do not appear to change the relative compatibility order of the three elements with respect to an anhydrous mantle (e.g., [44,56]). It is furthermore confirmed that all three elements behaved conservatively because any selective addition of Zr, Hf, or Lu to the mantle wedge by subduction components would displace a sample suite from this array. A very important observation is, however, that in Lu/Hf vs. Zr/Hf space (Fig. 4a), most Kamchatka samples are displaced to systematically lower Lu/Hf ratios than the global MORB array. As the Kamchatka samples overlap with compositions of global MORB in Zr vs. Zr/Hf space (Fig. 4b) and in Hf vs. Zr/Hf space (not shown), the difference between both magma types is clearly caused by a systematic deficit of Lu in the Kamchatka magmas. The Lu deficit cannot be attributed to the higher degrees of partial melting in the Kamchatka mantle wedge (10–20%) because at $D_{Lu}/D_{Zr,Hf} > 1$, an even larger depletion in Zr–Hf abundances relative to MORB would be expected. Likewise, systematically different degrees of mantle depletion in the sources of MORB and the Kamchatka arc rocks can also be ruled out. In this case, both groups should be clearly distinguishable in their Lu/Hf and Zr/Hf ratios because the two ratios are inversely correlated during mantle melting (Fig. 4a). In fact, the Kamchatka samples cover ca. 2/3 of the entire range in Zr/Hf and Lu/Hf ratios that are displayed in global MORB. Consequently, the Lu deficit is the consequence of higher $D_{Lu}/D_{Zr,Hf}$ during melting of the Kamchatka mantle wedge compared with MORB melting. The higher $D_{Lu}/D_{Zr,Hf}$ can be caused by (1) a higher $D_{Lu}/D_{Zr,Hf}$ in hydrous melting regimes or (2) by a higher average depth of the melting column, involving larger amounts of residual garnet and high pressure clinopyroxene. Experimental evidence indicates that the $D_{Lu}/D_{Zr,Hf}$ for clinopyroxene in mafic systems overlap between anhydrous ($D_{Lu}/D_{Hf} = 1.7–2.7$ [49,50,57]) and hydrous regimes ($D_{Lu}/D_{Hf} = 1.8–3.2$ [51]). Hence, the critical parameter is the higher average depth of the melting column beneath Kamchatka, where the lithosphere is thicker

than above MORB sources. At higher average melting depths, proportionally larger amounts of high pressure clinopyroxene or garnet (higher $D_{Lu}/D_{Hf}$, e.g., [50,55,58]) are involved during melting. This model is confirmed by the high $Ca_{6.0}$ and $Na_{6.0}$ in Kamchatka magmas [30] that are explained by the high crustal thickness (ca. 30 km [59]). Consistent with this explanation, we find that three samples from the Shmidt and Gamchen volcanoes, where the mantle wedge (and the melting column) is shallower (only 100 km [30]), overlap with global MORB in Lu/Hf vs. Zr/Hf space.

The NCKD and western Aleutian magmas are displaced to lower Lu/Hf ratios from the array defined by all other Kamchatka suites in Fig. 4a. Samples from the western Aleutians display the largest displacement. Together with high Sr/Y ratios (Fig. 6a), the low Lu/Hf ratios in the NCKD melts support previous models that, by analogy to the western Aleutians, significant amounts of slab melts were added to the sources of theses magmas [30,39,42]. The characteristically high Sr/Y and low Lu/Hf ratios in the slab melts originate from the presence of eclogite or garnet-amphibolite in the residual subducted oceanic crust where residual garnet retains the HREE and Y (e.g., [60–62]). Hence, the observed displacement of the NCKD samples from all other Kamchatka samples in Lu/Hf vs. Zr/Hf space (Fig. 4a) reflects a contribution of Zr–Hf from subduction components (adakitic melts). As observed for $^{176}Hf/^{177}Hf$ (Fig. 3c), the Zr/Hf ratio in the added adakitic melt must be similar to that in the CKD/EVF magmas because only a small increase of Zr/Hf with increasing Sr/Y is observed (Fig. 6b).

In summary, Zr, Hf, and the HREE all display conservative properties in the fluid-dominated subduction regime beneath Kamchatka, consistent with earlier models (e.g., [8,9,18]). Combined Zr–Hf–Lu systematics confirm a compatibility order of Zr < Hf < Lu in hydrous melt regimes. $D_{Lu}/D_{Hf}$ in the Kamchatka mantle wedge is higher than in the mantle sources of MORB because of the higher average depth of the melting column. In the mantle regimes where slab melts are present (western Aleutians, NCKD), the Zr–Hf–Lu budget is affected by the added slab melts. A similar Zr/Hf ratio in the slab melt component to those of global MORB (30–45 [44,45], however, rules out a significant

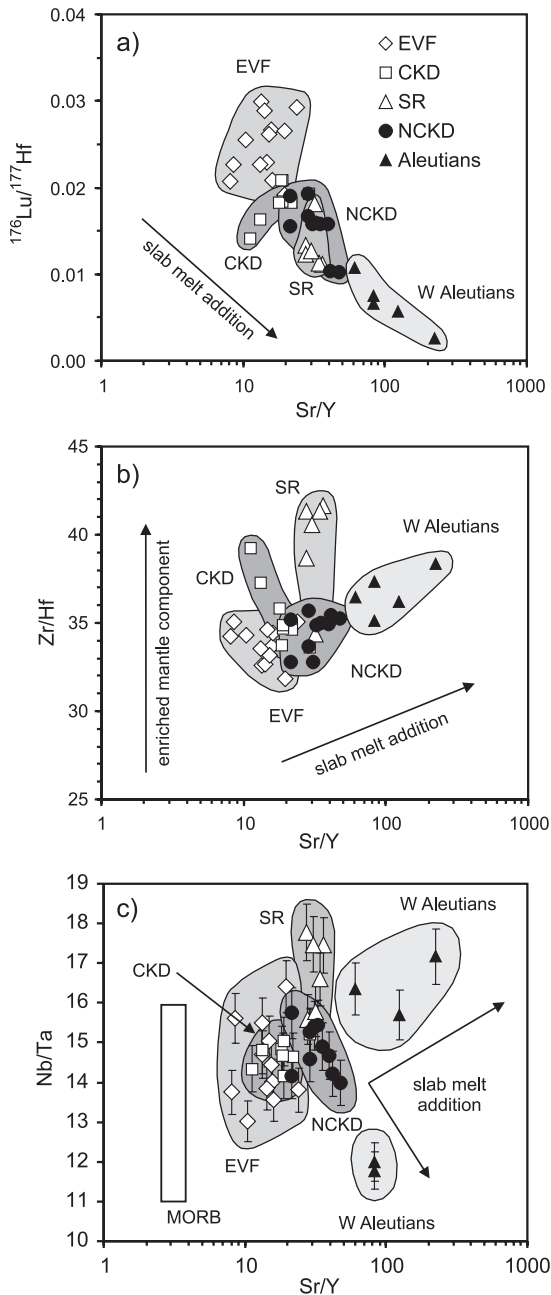Fig. 6. Plots of (a) Lu/Hf vs. Sr/Y, (b) Zr/Hf vs. Sr/Y, and (c) Nb/Ta vs. Sr/Y. Vectors indicate the effect of slab melt addition (=increase in Sr/Y) on the Lu/Hf, Zr/Hf and Nb/Ta ratios in the magmas. Note that the enriched mantle component in the source of the SR magmas is distinguished from the slab melts by a coupled increase of Nb/Ta and Zr/Hf and decrease of Lu/Hf at constant Sr/Y. Average MORB compositions are after [78] (Sr/Y) and [34,45] (Nb/Ta).

fractionation of the Zr/Hf ratio during slab melting processes.

### 4.3. Properties of Nb–Ta

The elements Nb and Ta are regarded as some of the most immobile in subduction fluids (e.g., [1,8,9]). Hence, Nb/Ta ratios in fluid-dominated subduction rocks should only be controlled by the mantle wedge composition. This is also supported by a previously reported strong correlation of Nb/Ta ratios with Nb concentrations in arc rocks (e.g., [22,24]). Because Nb is more incompatible than Ta during clinopyroxene controlled melting processes ($D_{Nb}/D_{Ta}$ ca. 0.3–0.8 in clinopyroxene, Fig. 7a), the observed correlation of Nb/Ta ratios with Nb concentrations has been interpreted to reflect variable degrees of mantle wedge depletion. If this is the case, then strong correlations of Nb/Ta ratios with other depletion parameters (e.g., Zr/Nb, Zr/Hf, Lu/Hf) are also expected. However, in Kamchatka rocks from the EVF, CKD, and NCKD, Nb/Ta ratios are not correlated with Lu/Hf, Zr/Hf or Zr/Nb ratios (e.g., Fig. 4c), showing that Nb/Ta is controlled by a different process. Only the SR samples, where an enriched mantle component is present, display higher Nb/Ta ratios at systematically lower Zr/Nb ratios and higher Zr/Hf ratios. Altogether, these observations imply that in the more enriched samples (SR and partly CKD) the budget of Nb–Ta is controlled by the mantle wedge. In the NCKD, western Aleutians, and to a small extent in the EVF, some of the Nb–Ta has been added to the mantle wedge by slab-derived components. The amount of added Nb–Ta, however, is only very small (up to a factor of ca. 2 relative to the mantle wedge contribution) as indicated by the high Zr/Nb in the Kamchatka samples that are comparable to those in MORB. This observation indicates that the contribution of Nb–Ta by subduction components is relevant in (1) the samples that originate from the most depleted mantle wedge (EVF) and (2) the samples with sources where slab melts are involved (NCKD, Aleutians).

From Nb/Ta ratios in samples where the Nb–Ta is largely contributed by slab components, it is possible to obtain insights into processes that may fractionate Nb from Ta during slab dehydration and melting processes. The fluid-dominated EVF rocks display considerable Nb/Ta variations (13.0–16.4) of which
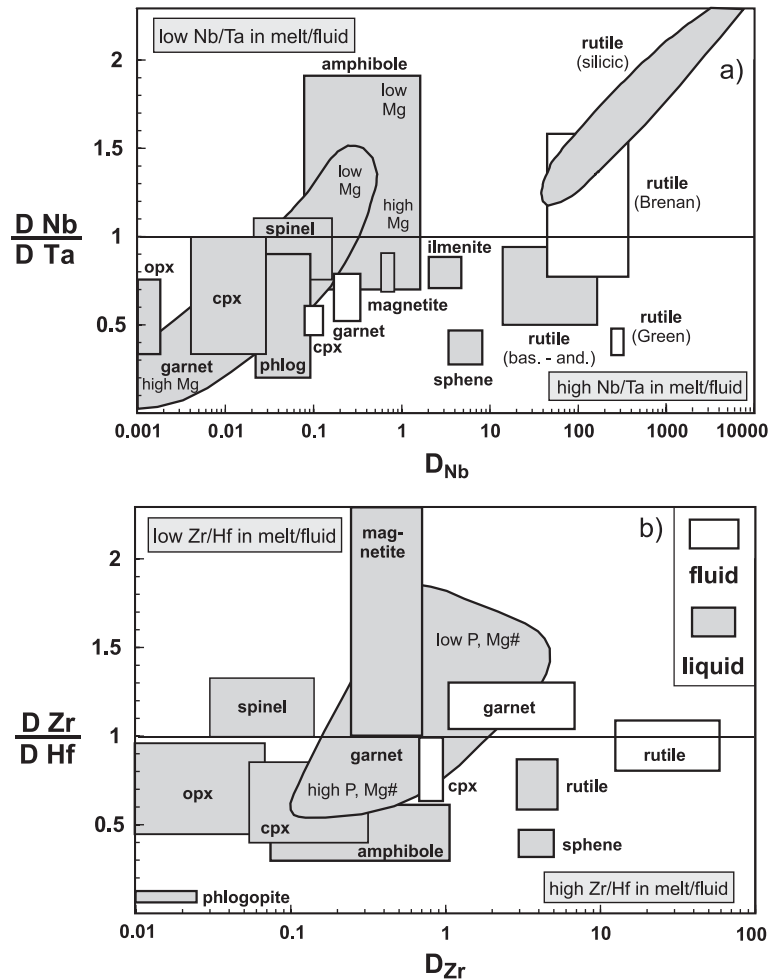
Fig. 7. Partition coefficients for Nb–Ta (a) and Zr–Hf (b) in major minerals occurring in mantle rocks, basalts, eclogites and amphibolites, updated after [35] and references therein. Other data sources for mineral-melt systems are clinopyroxene [28,49–51,57,62,79,80], orthopyroxene [51,81], garnet [28,51,57,69,82], amphibole [13,83–87], rutile [15,27,72,73], ilmenite and sphene [72,73], magnetite [72,88,89], spinel [90], phlogopite [51,84,91,92]. Data sources for mineral-fluid systems are: garnet and cpx [11], rutile [11,14,68].

the highest Nb/Ta ratios plot outside or at the upper limit of the MORB field in Nb/Ta vs. Zr/Hf space (Fig. 4c). If the lower Nb/Ta ratios (13–14) are assumed to reflect mantle wedge compositions, the Nb/Ta ratio in the added slab fluids must have been at least 16. This minimum Nb/Ta estimate is still within the range of present day MORB or OIB (MORB: 11–16 [45]; OIB: 15–17 [63]) which constitute the major source of subduction fluids beneath the Kamchatka arc. Hence, there is no evidence from the EVF data, that Nb was significantly fractionated from Ta during dehydration of the subducted oceanic crust. In similar

fashion as above, the Nb/Ta compositions of the NCKD and western Aleutian samples with the highest amounts of added slab melt (i.e., high Sr/Y) can be used to constrain the possible Nb/Ta fractionation during slab melting. In high Sr/Y samples of these two suites (Sr/Y>30, Fig. 6), the Nb/Ta ratios span a wide range between 11 and 17 (Fig. 6c). Some of these Nb/Ta ratios plot outside the range observed in MORB (Fig. 4c) which constitutes the most likely source of the slab melts. It is noteworthy that, in contrast to Zr/Hf (Fig. 6b), there are clearly resolvable groups of Aleutian samples with distinct Nb/Ta ratios

($\sim$ 12 and $\sim$ 16, respectively, Fig. 6c). The implications of this observation with respect to the petrological processes active during slab melting are discussed below.

The elevated Nb/Ta ratios (up to 18) found in rocks from the SR can provide constraints on the origin of the enriched mantle component beneath the Kamchatka bck-arc. As evident from Hf–Nd relationships, the trace element enrichment is best explained by the presence of either (1) an OIB-type asthenospheric source or (2) older enriched mantle lithosphere. Recent high precision measurements of Nb/Ta ratios in OIBs revealed a range in Nb/Ta of 15–17 [63], whereas magmas with a lithospheric mantle component in their source may display substantially higher Nb/Ta ratios (up to 19 [64]). Although the highest Nb/Ta ratios in the SR magmas are only slightly outside the OIB range, this tentatively suggests that subcontinental mantle lithosphere is a magma source beneath the Kamchatka back-arc region.

In summary, Nb/Ta systematics in the Kamchatka rocks show that Nb and Ta can be transported to the mantle wedge in both slab melts and fluids. In agreement with previous observations, the transport of Nb–Ta by slab fluids is rather limited and becomes only evident in the case of extremely depleted mantle wedge compositions. From the Kamchatka data, there is no evidence that the Nb/Ta ratio is fractionated during slab dehydration processes. There is, however, some indication that the Nb/Ta ratio may be fractionated during slab melting. Nb/Ta ratios may serve as a useful discriminant between plume and continental-lithosphere derived components in the sources of arc magmas.

## 4.4. Petrologic control of Nb/Ta and Zr/Hf ratios during slab melting and dehydration

Although arc magmas, MORB, and OIB have different abundances of HFSE, their Nb/Ta and Zr/Hf ratios are essentially identical. Any successful petrological model for slab melting and dehydration processes has to explain why these large concentration differences are not linked to larger Nb/Ta and Zr–Hf fractionations. A survey of published Nb–Ta and Zr–Hf partition coefficients for minerals present in mantle peridotite, eclogite, and garnet amphibolite is shown in Fig. 7. Rutile, amphibole and, to a lesser extent,

garnet and clinopyroxene are capable of controlling the Nb–Ta and Zr–Hf budget during melting and dehydration of subducted oceanic crust. Trace element budgets of eclogites and garnet amphibolites (e.g., [15,37,65–67]) confirm this observation and additionally propose metamorphic zircon to constitute an important host for Zr and Hf. All of these studies have identified rutile as the major host for Nb and Ta. Using the Kamchatka/Aleutian data, we evaluate the relative importance of these minerals during slab melting and dehydration processes. Any information about the behaviour of the HFSE in subduction fluids is restricted to Nb–Ta in the sources of the EVF magmas. The Nb/Ta ratio in the subduction fluids must be 16 or higher. Mineral-fluid partitioning experiments (e.g., [11]) indicate that $D_{Nb}/D_{Ta}$ in garnet and clinopyroxene is <1, consistent with a slightly elevated Nb/Ta ratio in slab fluids. There is presently no consensus, however, on the $D_{Nb}/D_{Ta}$ for rutile-fluid systems for which both $D_{Nb}/D_{Ta}$>1 and <1 were reported [14,68]. Hence, further experimental data are required for an in-depth evaluation of fluid-related processes. For the discussion of slab melting processes, we focus on a subset of adakitic samples from the W. Aleutians and the NCKD (Sr/Y>30) where the HFSE budget is interpreted as being predominantly controlled by slab melt components.

With increasing Sr/Y between the NCKD and W. Aleutian samples, the Zr/Hf ratios only show a slight increase from $\sim$ 35 up to 38 (Fig. 6b). Although the Zr/Hf ratio in the source of the slab melts is not precisely known, it can be assumed to be similar to the average MORB value (ca. 32–38; [34,45] and [44] corrected for spike bias, see [32]). The Zr/Hf ratios in the slab melts are therefore indistinguishable from those of average MORB, implying that the solidus phases in the subducting plate have a bulk $D_{Zr}/D_{Hf}$ that is close to unity. Experimentally derived $D_{Zr}/D_{Hf}$ for rutile/melt are $\sim$ 0.6 to $\sim$ 0.9 (e.g., [15,27]), showing that rutile was not a major host for Zr–Hf. For clinopyroxene and amphibole, experimentally derived $D_{Zr}/D_{Hf}$ for tonalitic (adakitic) systems are <1 (references in Fig. 7). In garnet, the experimentally derived $D_{Zr}/D_{Hf}$ are dependant on pressure and the MgO content of the garnets, increasing from $\sim$ 0.6 to $\sim$ 1.7 with decreasing MgO content and pressure (e.g., [51,69]). [55,70] used these experimental data to model the composition of slab derived tonalitic

melts as a function of the modal garnet/clinopyroxene ratio in the eclogitic residue. At a modal ratio of around 50:50, little fractionation of the Zr/Hf ratio is expected because the contrasting $D_{Zr}/D_{Hf}$ in clinopyroxene and garnet cancel each other out. Hence the observed lack of Zr/Hf fractionation in the western Aleutian and NCKD samples relative to MORB is well explained by a 50:50 mixture of residual clinopyroxene (alternatively amphibole) and garnet. Metamorphic zircon could also have controlled the Zr–Hf budget (see also [67]). [71] report that except for highly aluminous felsic melts zircon is not fractionating Zr/Hf ratios in magmatic systems.

In Nb/Ta vs Zr/Hf space (Fig. 4c) some of the adakitic samples plot outside the MORB field, showing that Nb can be fractionated from Ta to some extent during melting processes in subducting oceanic crust. Clinopyroxene and low-Mg garnet in tonalitic systems are unlikely to produce this fractionation because they have opposite $D_{Nb}/D_{Ta}$ that are close to unity (Fig. 7a and [70]). Major candidates to fractionate Nb from Ta in eclogites or garnet-amphibolites are residual rutile [27,72] and low Mg-amphibole [13,37] (Fig. 7a). Except for highly siliceous melts [73], the presence of rutile on the solidus would cause higher Nb/Ta ratios in coexisting melts. In contrast, low Mg-amphibole in garnet-amphibolite would cause lower Nb/Ta ratios in coexisting melts [13,37]. Nb/Ta ratios are therefore a powerful discriminant to assess the relative importance of amphibole and rutile during slab melting [37]. Fig. 8 illustrates the correlations of Nb/Ta and Nb/La ratios with Zr/Sm ratios in the high Sr/Y samples. Because of the high $D_{Zr,Nb}/D_{REE}$ in rutile [15], Nb/La and Zr/Sm are expected to correlate positively if rutile is in control whereas the presence of low Mg-amphibole (high $D_{Nb}/D_{La}$ and low $D_{Zr}/D_{Sm}$ [37]) would cause these ratios to be inversely correlated. The negative correlation of Nb/Ta with Zr/Sm (Fig. 8a) in the NCKD and western Aleutian samples shows that both end member assemblages are present in the magma sources. This observation is consistent with the slight increase of Zr/Hf with Sr/Y (Fig. 6b) because $D_{Zr}/D_{Hf}$ in rutile and amphibole are both < 1. A decrease of Nb/La with Zr/Sm in Fig. 8b, however, indicates that the variation of the negative HFSE anomalies is predominantly controlled by rutile and not by amphibole. Some amphibole must be present in all melt sources, however, because the
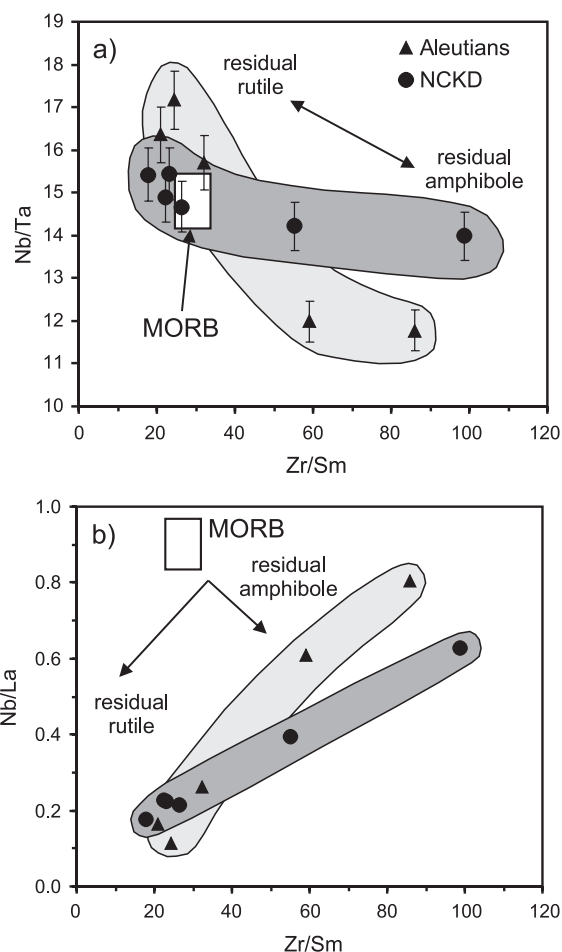


Fig. 8. Plots of Nb/Ta vs. Zr/Sm (a) and Nb/La vs. Zr/Sm (b) for samples with Sr/Y>30 where HFSE abundances are clearly controlled by the slab melt component. Average MORB compositions are after [78] (Nb/La, Zr/Sm) and [34,45] (Nb/Ta).

Aleutian and NCKD trends do not overlap with the Nb/La and Zr/Sm of average MORB (Fig. 8b). The apparently variable proportions of amphibole and rutile in the sources of the slab melts may reflect different P–T conditions, degrees of melting or different $TiO_2$ contents of the protoliths [70].

In summary, the Kamchatka end member case provides some insights into the processes that deplete the HFSE in slab fluids where no mobility of Zr–Hf and little mobility of Nb–Ta were observed. Because a sediment component is absent in the magmas, it can be shown that water-rich fluids and their residual minerals in subducted oceanic crust do

not fractionate the Nb/Ta ratio in a measurable way. However, during melting of subducted oceanic crust, amphibole and rutile are the predominant phases controlling the Nb and Ta budget, causing small but resolvable Nb/Ta fractionations. The budget of Zr and Hf is best explained by ~ 50:50 assemblages of clinopyroxene/amphibole and garnet or by meta-morphic zircon.

## 5. Conclusions

High precision HFSE concentration data together with Hf–Nd isotope relationships in Kamchatka arc rocks provide the following constraints on the behav-iour of HFSE during subduction zone processes:

(1) The isotope compositions of Hf and Nd in Kamchatka arc rocks indicate that the "Indian type" mantle domain is present in the NW. Pacific region and forms the Kamchatka subarc mantle wedge, similar as previously reported for the Izu–Bonin and Mariana arcs [18].
(2) In the fluid-dominated subduction regime beneath Kamchatka (EVF, CKD, SR), Lu, Zr, and Hf behave conservatively, whereas small amounts of the Nb–Ta were added by subduction fluids. The amount added, however, is insignificant with respect to typical mass balance calculations for subduction systems that frequently rely on the immobility of Nb.
(3) In the melt-dominated subduction regime beneath Kamchatka (NCKD) and the western Aleutians, all HFSE behave nonconservatively.
(4) From the Kamchatka data, there is no clear evidence that Nb/Ta and Zr/Hf ratios are frac-tionated at a globally significant scale during subduction processes. The presence of residual amphibole and rutile during slab melting may cause some fractionation of Nb and Ta. Both minerals, however, produce opposite fraction-ation trends which might cancel each other out at a global scale. Further high-precision measure-ments of Nb/Ta and Zr/Hf ratios in Archean TTG suites can help to test models that explain the low Nb/Ta ratio of the continental crust (ca. 12 [74]) by the presence of amphibole in subducting oceanic crust during Archean crustal growth

(e.g., [37]). At present, subduction processes appear to be an unlikely explanation for the Nb/Ta paradox, i.e., the observation that all accessible silicate reservoirs on Earth display Nb/Ta ratios that are below the chondritic ratio of $19.9 \pm 0.6$ [34]. The data therefore lend further support to the experimental prediction that some of the Nb is hosted by the Earth's core [75]. The absence of any resolvable Zr/Hf fractionation during slab melting processes beneath Kamchatka confirms that there is no globally significant fractionation of this element ratio during subduction processes, thus explaining the previously reported lack of Zr/Hf fractionation during formation of continental crust (e.g., [56,74]).

## Acknowledgements

## References

[1] J.W. Pearce, D.W. Peate, Tectonic implications of the compo-sition of volcanic arc magmas, Annu. Rev. Earth Planet. Sci. 23 (1995) 251–285.

[2] A.E. Ringwood, The petrological evolution of island arc sys-tems, J. Geol. Soc. (Lond) 130 (1974) 183–204.

[3] S.M. Peacock, T. Rushmer, A.B. Thompson, Partial melting of subducting oceanic crust, Earth Planet. Sci. Lett. 121 (1994) 227–244.

[4] P.B. Kelemen, J.L. Rilling, E.M. Parmentier, L. Mehl, B.R. Hacker, Thermal structure due to solid-state flow in the mantle wedge beneath arcs, in: J. Eiler (Ed.), Inside the Subduction Factory, AGU Geophys. Monogr. vol. 138, 2004, pp. 324, AGU.

[5] M.S. Drummond, M.J. Defant, A model for trondhjeimite–tonalite–dacite genesis and crustal growth via slab melting: archean to modern comparisons, J. Geophys. Res. 95 (B13) (1990) 21503–21521.

[6] G.M. Yogodzinski, R.W. Kay, O.N. Volynets, A.V. Koloskov, S.M. Kay, Magnesian andesite in the western Aleutian

Komandorsky region: implications for slab melting and processes in the mantle wedge, Bull. Geol. Soc. Am. 107 (1995) 505–519.

[7] G.T. Nichols, P.J. Wyllie, C.R. Stern, Subduction zone melting of pelagic sediments constrained by melting experiments, Nature 371 (1994) 785–788.

[8] M.T. McCulloch, J.A. Gamble, Geochemical and geodynamical constraints on subduction zone magmatism, Earth Planet. Sci. Lett. 102 (1991) 358–374.

[9] H. Keppler, Constraints from partitioning experiments on the composition of subduction-zone fluids, Nature 380 (1996) 237–240.

[10] J.M. Brenan, H.F. Shaw, F.J. Ryerson, D.L. Phinney, Mineral-aqueous fluid partitioning of trace elements at 900 °C and 2.0 GPa: constraints on the trace element geochemistry of mantle and deep crustal fluids, Geochim. Cosmochim. Acta 59 (1995) 3331–3350.

[11] R. Stalder, S.F. Foley, G.P. Brey, I. Horn, Mineral-aqueous fluid partitioning of trace elements at 900–1200 °C and 3.0–5.7 GPa: new experimental data for garnet, clinopyroxene, and rutile, and implications for mantle metasomatism, Geochim. Cosmochim. Acta 62 (10) (1998) 1781–1801.

[12] D.A. Ionov, A.W. Hofmann, Nb–Ta-rich mantle amphiboles and micas: implications for subduction related metasomatic trace element fractionation, Earth Planet. Sci. Lett. 131 (1995) 341–356.

[13] M. Tiepolo, R. Vannucci, R. Oberti, S. Foley, P. Bottazzi, A. Zanetti, Nb and Ta incorporation and fractionation in titanian pargasite and kaersutite: crystal chemical constraints and implications for natural systems, Earth Planet. Sci. Lett. 176 (2) (2000) 185–201.

[14] J.M. Brenan, H.F. Shaw, D.L. Phinney, F.J. Ryerson, Rutile-aqueous fluid partitioning of Nb, Ta, Hf, Zr, U and Th: implications for high field strength element depletions in island-arc basalts, Earth Planet. Sci. Lett. 128 (1994) 327–339.

[15] S.F. Foley, M.G. Barth, G.A. Jenner, Rutile/melt partition coefficients for trace elements and an assessment of the influence of rutile on the trace element characteristics of subduction zone magmas, Geochim. Cosmochim. Acta 64 (2000) 933–938.

[16] F.J. Ryerson, E.B. Watson, Rutile saturation in magmas: implications for Ti–Nb–Ta depletion in island arc basalts, Earth Planet. Sci. Lett. 86 (1987) 225–239.

[17] W.M. White, P.J. Patchett, Hf–Nd–Sr isotopes and incompatible element abundances in island arcs: implications for magma origin and crust mantle evolution, Earth Planet. Sci. Lett. 67 (1984) 167–185.

[18] J.A. Pearce, P.D. Kempton, G.M. Nowell, S.R. Noble, Hf–Nd element and isotope perspective on the nature and provenance of mantle and subduction components in Western Pacific arc-basin systems, J. Petrol. 40 (11) (1999) 1579–1611.

[19] J.D. Woodhead, J.M. Hergt, J.P. Davidson, S.M. Eggins, Hafnium isotope evidence for "conservative" element mobility during subduction processes, Earth Planet. Sci. Lett. 192 (2001) 331–346.

[20] V.J.M. Salters, S.R. Hart, The mantle sources of ocean ridges, islands and arcs: the Hf isotope connection, Earth Planet. Sci. Lett. 104 (1991) 364–380.

[21] M. Bizimis, V.J.M. Salters, E. Bonatti, Trace and REE content of clinopyroxenes from supra-subduction zone peridotites. Implications for melting and enrichment processes in island arcs, Chem. Geol. 165 (1–2) (2000) 67–85.

[22] S.M. Eggins, J.D. Woodhead, L.P.J. Kinsley, G.E. Mortimer, P. Sylvester, M.T. McCulloch, J.M. Hergt, M.R. Handler, A simple method for the precise determination of >40 trace elements in geological samples by ICPMS using enriched isotope internal standardisation, Chem. Geol. 134 (1997) 311–326.

[23] T. Elliot, T. Plank, A. Zindler, W.M. White, B. Bourdon, Element transport from subducted slab to volcanic front at the Mariana arc, J. Geophys. Res. 102 (B7) (1997) 14991–15019.

[24] T. Plank, W.M. White, Nb and Ta in arc and Mid Ocean Ridge basalts, Eos 76 (46) (1995) 655.

[25] C. Münker, Nb/Ta fractionation in a Cambrian arc/back arc system, New Zealand: source constraints and application of refined ICPMS techniques, Chem. Geol. 144 (1998) 23–45.

[26] M.F. Thirlwall, T.E. Smith, A.M. Graham, N. Theodoru, P. Hollings, J.P. Davidson, R.J. Arculus, High field strength anomalies in arc magmas: source or processes? J. Petrol. 35 (1994) 819–838.

[27] G.A. Jenner, S.F. Foley, S.E. Jackson, T.H. Green, B.J. Fryer, H.P. Longerich, Determination of partition coefficients for trace elements in high pressure–temperature experimental run products by laser ablation microprobe-inductively coupled plasma-mass spectrometry (LAM-ICP-MS), Geochim. Cosmochim. Acta 58 (1994) 5099–5103.

[28] E.H. Hauri, T.P. Wagner, T.L. Grove, Experimental and natural partitioning of Th, U, Pb and other trace elements between garnet, clinopyroxene and basaltic melts, Chem. Geol. 117 (1994) 149–166.

[29] R.W. Kay, Aleutian magnesian andesites: melts from subducted Pacific Ocean crust, J. Volcanol. Geotherm. Res. 4 (1978) 117–132.

[30] T. Churikova, F. Dorendorf, G. Wörner, Sources and fluids in the mantle wedge below Kamchatka, evidence from across-arc geochemical variation, J. Petrol. 42 (8) (2001) 1567–1593.

[31] C. Münker, S. Weyer, E.E. Scherer, K. Mezger, Separation of high field strength elements (Nb, Ta, Zr, Hf) and Lu from rock samples for MC-ICPMS measurements, Geochem. Geophys. Geosyst. 2 (2001) (paper number 10.1029/2001GC000183).

[32] S. Weyer, C. Münker, M. Rehkämper, K. Mezger, Determination of ultra-low Nb, Ta, Zr and Hf concentrations and the chondritic Zr/Hf and Nb/Ta ratios by isotope dilution analyses with multiple collector ICP-MS, Chem. Geol. 187 (2002) 295–313.

[33] K.P. Jochum, H.M. Seufert, B. Spettel, H. Palme, The solar system abundances of Nb, Ta and Y, and the relative abundances of refractory lithophile elements in differentiated planetary bodies, Geochim. Cosmochim. Acta 50 (1986) 1173–1183.

[34] C. Münker, J.A. Pfänder, S. Weyer, A. Büchl, T. Kleine, K. Mezger, Evolution of planetary cores and the Earth–Moon system from Nb/Ta systematics, Science 301 (2003) 84–87.

[35] T.H. Green, Significance of Nb/Ta as an indicator of geochemical processes in the crust mantle system, Chem. Geol. 120 (1995) 347–359.

[36] R.L. Rudnick, M. Barth, I. Horn, W.F. McDonough, Rutile-bearing refractory eclogites: missing link between continents and depleted mantle, Science 287 (2000) 278–281.

[37] S. Foley, M. Tiepolo, R. Vannucci, Growth of early continental crust controlled by melting of amphibolite in subduction zones, Nature 417 (2002) 837–840.

[38] A.G. Hochstaedter, P.K. Kepezhinskas, M.J. Defant, M.S. Drummond, H. Bellon, On the tectonic significance of arc volcanism in Northern Kamchatka, J. Geol. 102 (1994) 639–654.

[39] P.K. Kepezhinskas, F. McDermott, M.J. Defant, A. Hochstaedter, M.S. Drumond, C.J. Hawkesworth, A. Koloskov, R.C. Maury, H. Bellon, Trace element ans Sr–Nd–Pb isotopic constraints on a three component model of Kamchatka Arc Petrogenesis, Geochim. Cosmochim. Acta 61 (3) (1997) 577–600.

[40] F. Dorendorf, U. Wiechert, G. Wörner, Hydrated sub-arc mantle: a source for the Kluchevskoy volcano, Kamchatka/Russia, Earth Planet. Sci. Lett. 175 (2000) 69–86.

[41] G. Wörner, H.T. Churikova, W. Leeman, V. Liebetrau, S. Tonarini, A. Heuser, Fluid-mobile trace element and U-series isotope variations across Kamchatka: timing and effects of slab dehydration, Schr.reihe Dtsch. Geol. Ges. 14 (2001) 236–237.

[42] G.M. Yogodzinski, J.M. Lees, T. Churikova, F. Dorenforf, G. Wörner, O.N. Volynets, Geochemical evidence for the melting of subducting oceanic lithosphere at plate edges, Nature 409 (2001) 500–504.

[43] A.B. Kersting, R.J. Arculus, Pb isotope composition of Klyuchevskoy volcano, Kamchatka and North Pacific sediments: implications for magma genesis and crustal recycling in the Kamchatkan arc, Earth Planet. Sci. Lett. 136 (3–4) (1995) 133–148.

[44] K. David, P. Schiano, C.J. Allègre, Assessment of the Zr/Hf fractionation in oceanic basalts and continental materials during petrogenetic processes, Earth Planet. Sci. Lett. 178 (2000) 285–301.

[45] A. Büchl, C. Münker, K. Mezger, A.W. Hofmann, High precision Nb/Ta and Zr/Hf ratios in global MORB, Geochim. Cosmochim. Acta, Suppl. 66 (2002) A108.

[46] C. Chauvel, J. Blichert-Toft, A hafnium isotope and trace element perspective on melting of the depleted mantle, Earth Planet. Sci. Lett. 190 (2001) 137–151.

[47] J.D. Woodhead, Geochemistry of the Mariana arc (western Pacific): source composition and processes, Chem. Geol. 76 (1989) 1–24.

[48] G.A. Gaetani, T.L. Grove, The influence of water on melting of mantle peridotite, Contrib. Mineral. Petrol. 131 (1998) 323–346.

[49] S.R. Hart, T. Dunn, Experimental cpx/melt partitioning of 24 trace elements, Contrib. Mineral. Petrol. 113 (1993) 1–8.

[50] J.D. Blundy, J.A.C. Robinson, B.J. Wood, Heavy REE are compatible in clinopyroxene on the spinel lherzolite solidus, Earth Planet. Sci. Lett. 160 (1998) 493–504.

[51] T.H. Green, J.D. Blundy, J. Adam, G.M. Yaxley, SIMS determination of trace element partition coefficients between garnet, clinopyroxene and hydrous basaltic liquids at 2–7.5 GPa and 1080–1200 °C, Lithos 53 (2000) 165–187.

[52] J.A. Pearce, P.E. Baker, P.K. Harvey, I.W. Luff, Geochemical evidence for subduction fluxes, mantle melting and fractional crystallization beneath the South Sandwich island arc, J. Petrol. 36 (1995) 1073–1109.

[53] A. Ewart, K.D. Collerson, M. Regelous, J.I. Wendt, Y. Niu, Geochemical evolution within the Tonga–Kermadec–Lau arc-back-arc systems: the role of varying mantle wedge composition in space and time, J. Petrol. 39 (3) (1998) 331–368.

[54] J.A. Pearce, I.J. Parkinson, Trace element models for mantle melting: application to volcanic arc petrogenesis, in: H.M. Prichard, T. Alabaster, N.B. Harris, C.R. Neary (Eds.), Magmatic Processes and Plate Tectonics, Spec. Publ.-Geol. Soc. vol. 76, 1993, pp. 373–403.

[55] W. van Westrenen, J.D. Blundy, B.J. Wood, High field strength element/rare earth element fractionation during partial melting in the presence of garnet: implications for identification of mantle heterogeneities, Geochem. Geophys. Geosyst. (2) (2000) (Paper number 2000GC000133).

[56] S. Weyer, C. Münker, K. Mezger, Nb/Ta, Zr/Hf and REE in the depleted mantle: implications for the differentiation history of the crust–mantle system, Earth Planet. Sci. Lett. 205 (3–4) (2003) 309–324.

[57] K.T.M. Johnson, Experimental determination of partition coefficients for rare earth and high-field-strength elements between clinopyroxene, garnet and basaltic melt at high pressures, Contrib. Mineral. Petrol. 133 (1998) 60–68.

[58] P. McDade, J. Blundy, B.J. Wood, Trace element partitioning on the Tinaquillo lherzolite solidus at 1.5 GPa, Phys. Earth Planet. Inter. 139 (2003) 129–147.

[59] E.I. Gordeev, A.A. Gusev, V.E. Levin, V.F. Bakhtiarov, V.M. Pavlov, V.N. Chebrov, M. Kasahara, Preliminary analysis of deformation at the Eurasia–Pacific–North America plate junction from GPS data, Geophys. J. Int. 147 (1) (2001) 189–198.

[60] R.P. Rapp, E.B. Watson, Dehydration melting of metabasalt at 8–32 kbar: implications for continental growth and crust–mantle recycling, J. Petrol. 35 (1995) 891–931.

[61] H. Martin, Adakitic magmas: modern analogues of Archean granitoids, Lithos 46 (1999) 411–429.

[62] M.G. Barth, S.F. Foley, I. Horn, Partial melting in Archean subduction zones: constraints from experimentally determined trace element partition coefficients between eclogitic minerals and tonalitic melts under upper mantle conditions, Precam. Res. 113 (2002) 323–340.

[63] J.A. Pfänder, C. Münker, K. Mezger, A.W. Hofmann, In search of a superchondritic Nb/Ta reservoir: high precision Nb/Ta and Zr/Hf ratios in ocean island and intraplate basalts, Geochim. Cosmochim. Acta, Suppl. 66 (S1) (2002) A597.

[64] J.A. Pfänder, C. Münker, S. Jung, K. Mezger, Plume-lithosphere interaction: evidence from high-precision Nb/Ta and Zr/Hf ratios and Nd–Hf isotope systematics in volcanic rocks from Central Germany, Geophys. Res. Abstr. 5 (2003) 07400.

[65] S.S. Sorensen, J.N. Grossman, Enrichment of trace elements in garnet amphibolites from a paleo-subduction zone: Catalina Schist, southern California, Geochim. Cosmochim. Acta 53 (1989) 3155–3177.

[66] T. Zack, A. Kronz, S.F. Foley, T. Rivers, Trace element abundances in rutiles from eclogites and associated garnet mica schists, Chem. Geol. 184 (2002) 97–122.

[67] D. Rubatto, J. Hermann, Zircon formation during fluid circulation in eclogites (Monviso, Western Alps): implications for Zr and Hf budget in subduction zones, Geochim. Cosmochim. Acta 67 (12) (2003) 2173–2187.

[68] T.H. Green, New partition coefficient determinations pertinent to hydrous melting processes in subduction zones, State of the Arc 2000 Abstracts, IAVCEI, Ruapehu, 2000.

[69] W. van Westrenen, J. Blundy, B. Wood, Crystal-chemical controls on trace element partitioning between garnet and anhydrous silicate melt, Am. Mineral. 84 (1999) 838–847.

[70] S. Klemme, J.D. Blundy, B.J. Wood, Experimental constraints on major and trace element partitioning during partial melting of eclogite, Geochim. Cosmochim. Acta 66 (17) (2002) 3109–3123.

[71] R.L. Linnen, H. Keppler, Melt composition control of Zr/Hf fractionation in magmatic processes, Geochim. Cosmochim. Acta 66 (18) (2002) 3293–3301.

[72] T.H. Green, N.J. Pearson, An experimental study of Nb and Ta partitioning between Ti-rich minerals and silicate minerals at high pressure and temperature, Geochim. Cosmochim. Acta 51 (1987) 55–62.

[73] R.L. Linnen, H. Keppler, Culombite solubility in granitic melts: consequences for the enrichment and fractionation of Nb and Ta in the Earth's crust, Contrib. Mineral. Petrol. 128 (1997) 213–227.

[74] M.G. Barth, W.F. Mc Donough, R.L. Rudnick, Tracking the budget of Nb and Ta in the continental crust, Chem. Geol. 165 (2000) 197–213.

[75] J. Wade, B.J. Wood, The Earth's missing niobium may be in the core, Nature 409 (2001) 75–78.

[76] C.J. Hawkesworth, S. Turner, D. Peate, F. McDermott, P. van Calsteren, Elemental U and Th variations in island arc rocks: implications for U-series isotopes, Chem. Geol. 139 (1997) 207–221.

[77] P.D. Kempton, J.A. Pearce, T. Barry, J.G. Fitton, C. Langmuir, D.M. Christie, Sr–Nd–Pb–Hf isotope results from ODP leg 187: evidence for mantle dynamics of the Australian–Antarctic discordance and origin of the Indian MORB source, Geochem. Geophys. Geosyst. 3 (12) (2002) (paper number 2002GC000320).

[78] A.W. Hofmann, Chemical differentiation of the earth: the relationship between mantle, continental crust and oceanic crust, Earth Planet. Sci. Lett. 90 (1988) 297–314.

[79] C.C. Lundstrom, H.F. Shaw, F.J. Ryerson, Q. Williams, J. Gill, Crystal chemical control of clinopyroxene-melt partitioning in the Di–Ab–An system: implications for elemental fractionations in the depleted mantle, Geochim. Cosmochim. Acta 62 (16) (1998) 2849–2862.

[80] M. Klein, H.G. Stosch, H.A. Seck, N. Shimizu, Experimental partitioning of high field strength and rare earth elements between clinopyroxene and garnet in andesitic to tonalitic systems, Geochim. Cosmochim. Acta 64 (1) (2000) 99–115.

[81] A.K. Kennedy, G.E. Lofgren, G.J. Wasserburg, An experimental study of trace element partitioning between olivine, orthopyroxene and melt in chondrules; equilibrium values and kinetic effects, Earth Planet. Sci. Lett. 115 (1993) 177–195.

[82] V.J.M. Salters, J. Longhi, Trace element partitioning during the initial stages of melting beneath mid-ocean ridges, Earth Planet. Sci. Lett. 166 (1999) 15–30.

[83] J.M. Brenan, H.F. Shaw, F.J. Ryerson, D.L. Phinney, Experimental determination of trace element partitioning between pargasite and a synthetic hydrous andesitic melt, Earth Planet. Sci. Lett. 135 (1995) 1–11.

[84] T. LaTourette, R.L. Hervig, J.R. Holloway, Trace element partitioning between amphibole, phlogopite and basanite melt, Earth Planet. Sci. Lett. 135 (1995) 13–30.

[85] T. Zack, S.F. Foley, G.A. Jenner, A consistent partition coefficient set for clinopyroxene, amphibole, and garnet from laser ablation microprobe analysis of garnet pyroxenites from Kakanui, New Zealand, Neues Jahrb. Mineral. Abh. 172 (1) (1997) 23–41.

[86] M. Klein, H.G. Stosch, H.A. Seck, Partitioning of high field-strength and rare-earth elements between amphibole and quartz-dioritic to tonalitic melts: an experimental study, Chem. Geol. 138 (1997) 257–271.

[87] M. Hilyard, R.L. Nielsen, J.S. Beard, A. Patino-Douce, J. Blencoe, Experimental determination of the partitioning behavior of rare earth and high field strength elements between pargasitic amphibole and natural silicate melts, Geochim. Cosmochim. Acta 64 (6) (2000) 1103–1120.

[88] P. Beattie, The effect of partial melting of spinel peridotite on uranium series disequilibria: constraints from partitioning studies, Earth Planet. Sci. Lett. 177 (1993) 379–391.

[89] G.A. Mahood, E.W. Hildreth, Large partition coefficients for trace elements in high-silica rhyolites, Geochim. Cosmochim. Acta 47 (1980) 11–30.

[90] I. Horn, S.F. Foley, S.E. Jackson, G.A. Jenner, Experimentally determined partitioning of high field strength-and selected transition elements between spinel and basaltic melt, Chem. Geol. 117 (1994) 193–218.

[91] S.F. Foley, S.E. Jackson, B.J. Fryer, J.D. Greenough, G.A. Jenner, Trace element partition coefficients for clinopyroxene and phlogopite in an alkaline lamprophyre from Newfoundland by LAM-ICP-MS, Geochim. Cosmochim. Acta 60 (1996) 629–638.

[92] K.H. Schmidt, P. Bottazzi, R. Vannucci, K. Mengel, Trace element partitioning between phlogopite, clinopyroxene and leucite lamproite melt, Earth Planet. Sci. Lett. 168 (1999) 287–299.

[93] J. Blichert-Toft, F. Albarède, The Lu–Hf isotope geochemistry of chondrites and the evolution of the mantle–crust system, Earth Planet. Sci. Lett. 148 (1997) 243–258.

[94] S.B. Jacobsen, G.J. Wasserburg, Sm–Nd isotopic evolution of chondrites, Earth Planet. Sci. Lett. 50 (1980) 139–155.